Energy, Mines and Resources Canada | Énergie, Mines et Ressources Canada

CANMET

Canada Centre for Mineral and Energy Technology | Centre canadien de la technologie des minéraux et de l'énergie

DECLASSIFIED
D... NOV 29 1982
AUTHORIZED

EXAMINATION OF STEEL FROM TWO FAILURES IN THE GRIZZLY SOUR-GAS PIPELINE

G.J. BIEFER AND M. FICHERA
CORROSION SCIENCE SECTION

MARCH 1982

MINERALS RESEARCH PROGRAM

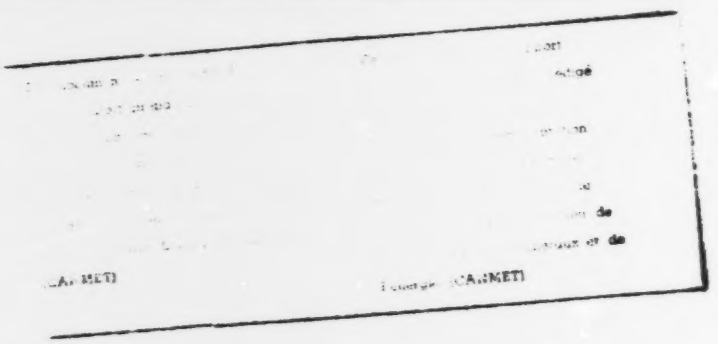

55 pp

PHYSICAL METALLURGY RESEARCH LABORATORIES
REPORT MRP/PMRL 82-3 (CF)

MAR 15 1985
MICROMEDIA

85-2539/

DECLASSIFIED
NOV 29 1982

PHYSICAL METALLURGY RESEARCH LABORATORIES
REPORT MRP/PMRL 82-3 (CF)

EXAMINATION OF STEEL FROM TWO FAILURES IN THE GRIZZLY SOUR-GAS PIPELINE

by

G.J. Biefer and M. Fichera

INTRODUCTION

Physical Metallurgy Research Laboratories (PMRL) were requested by the National Energy Board (NEB) to examine samples taken from pipe in the vicinity of two pipeline failures which occurred in Westcoast Transmission Company's Grizzly (sour gas) Pipeline in British Columbia during July, 1981 (Appendix I). NEB requested an interim report describing the observations and findings of the PMRL laboratory examination, and a summary of the probable causes of the failures; this has been supplied (1).

NEB provided a short summary of information on the Grizzly Pipeline failures (Appendix II), a number of mounted metallographic sections, and pieces cut from the pipe wall. They were accompanied by drawings giving the locations of the steel samples relative to the pipe fractures, and by chemical analyses of the samples (Appendix III and Appendix IV).

In brief, Grade 359 spiral-weld 508 x 9.5 mm pipe had failed after about 17-months service in sour (~27.5% H_2S) natural gas at an operating pressure of 6-7 MPa. Fractures had occurred in the weld and in the weld HAZ.

It is well known that steel components, under tensile stress in a wet, H_2S-containing environment, can fail by "sulphide stress cracking" (SSC). A compilation of classic papers on H_2S corrosion, including SSC, has been recently published (2). Comprehensive reviews on SSC are available (3,4). Factors affecting a related form of H_2S cracking damage termed "stepwise cracking" (SWC) have also been reviewed (5), and recent publications discuss and compare SSC and SWC in pipelines (6,7,8,9).

The present report provides a detailed description of the observations and findings of the PMRL examination of samples of line-pipe steel from the failed Grizzly Pipeline. It is important to note that this examination has been limited to the samples supplied. All conclusions are based on these samples and on the information provided by NEB, appended to this report.

FAILURE NO. 1

The first of the two failures on the Grizzly Pipeline occurred on July 20, 1981. The location of samples taken from pipe in the vicinity of the fracture is indicated in Appendix III. The eleven samples listed in Table 1 were supplied to PMRL as polished and etched mounted metallographic sections through the pipe wall. Three pieces about 200 x 150 mm, flame-cut from the pipe wall near the failure, were also made available (Figs. 1, 2, and 3). The lower edge of piece 982-A-2, as shown in Fig. 2, was part of the major fracture surface at the pipeline failure, and was stated by NEB to be adjacent to the failure initiation zone.

FAILURE NO. 2

The second failure of the Grizzly Pipeline took place on July 27, 1981. The location of samples taken from pipe near the failure is shown in Appendix IV. The seven samples listed in Table 2 were supplied to PMRL as polished and etched mounted metallographic sections through the pipe wall. Appendix IV indicates that the five metallographic sections from pipe section A-2 were all taken near the major fracture surface at the pipeline failure.

EXAMINATION OF SPECIMENS

METALLOGRAPHIC SECTIONS

The sections through the pipe wall taken in connection with both failures showed scaling, corroded surfaces on the inside of the pipe. This was also observed in the larger pieces cut from the pipe wall, as shown in Fig. 1-3.

The majority of the metallographic sections listed in Tables 1 and 2 showed cracks which had initiated on the corroded inside pipe surfaces and generally had propagated in the through-thickness direction. All the cracks were associated with spiral welds, and fell into three main categories:

1. "WT" cracks in weld metal, transverse to the weld direction;
2. "WL" cracks in weld metal, and in the weld direction;
3. "HL" cracks parallel to the weld in the HAZ.

Tables 1 and 2 indicate the type and number of major cracks on the as-received metallographic sections and the three pieces of pipe wall. Most cracks had penetrated at least halfway through the pipe wall, and some had penetrated right through. The results of the examination of the metallographic sections follow.

(1) Failure 1

As shown in Table 1, WT, WL and HL cracks were identified. Examination of metallographic sections of cracks partly through the pipe wall, using an optical microscope, showed deposits of corrosion product within the cracks. The deposits were still visible very close to the crack tips.

A WL crack is shown in Fig. 4. Corrosion has widened the part of the crack in the first (inside) weld pass, and shallow pits, microcracks and corrosion product were seen within this corroded part of the crack. A view at higher magnification is given in Fig. 5.

Figure 6 shows a HL crack which was typical of all such cracks observed in having initiated in the coarse-grained HAZ, very close to the weld fusion zone. Figure 7 shows the tip of this crack at higher magnification. A tendency towards SWC in this part of the crack is manifested in the form of abrupt bends and short branches lying more or less in the plate rolling plane. The appearance of this crack profile may be contrasted with the classical SSC in weld metal shown in Fig. 9; weld metal is immune from SWC (5). In Fig. 7 there are also a few small stepwise cracks in the immediate vicinity of, but apparently not connected to, the main crack. One of these, to be seen below the main crack tip, shows distinct steps.

Similar indications of SWC were shown by some - though not all - portions of cracks lying in the fine-grained HAZ, and they were most evident in the middle third of the pipe wall. On the other hand, SWC was never associated with the initiation of HL cracks, and it did not occur at locations remote from the main cracks.

Figure 8 shows three adjacent WL cracks in the same weld bead. One has penetrated through the pipe wall. Near the apparent origin of the through-crack on the inner weld face, an examination at higher magnification

shows mechanical deformation of metal and microstructure at crack surfaces. Examples of mechanical deformation are shown in connection with Failure 2 in Fig. 14 and 15. In the through-crack in Fig. 8, there are signs of corrosion on crack surfaces at a greater depth than the mechanically deformed region. This suggests that environmentally-assisted cracking has by-passed and undercut a ligament of sound metal which has later fractured mechanically. Figure 9 shows the tip of one of the part-through cracks of Fig. 8, at the interface between the two weld passes.

The longitudinal weld section in Fig. 10 shows a WT crack which has penetrated through the inner and into the outer weld pass. A 2.5 mm long, dark, oval ring at the crack origin appeared when the section was etched with 2 1/2% nital. At the right-hand side of the ring, as shown in Fig. 11, a micro-crack has developed, and what appear to be dark second-phase precipitates are visible. The results of microhardness measurements, given later, identified the dark, oval ring as a hard spot.

(2) Failure 2

As indicated in Table 2, HL cracks were the most common type in Failure 2, and these had all initiated at the interface between the weld fusion zone and the weld HAZ. All major cracks had propagated through the pipe wall.

A typical HL crack is shown in Fig. 12. Examination at higher magnification of crack surfaces at the presumed origin, inside the pipe, showed signs of corrosion. As shown in Fig. 13, corrosion was characterized by an irregular, indented profile and short secondary microcracks. Such corroded surfaces extended halfway through the pipe wall; beyond, crack surfaces became straighter, and showed distorted microstructure and distorted metal indicative of a mechanical cracking mechanism, as shown in Fig. 14 and 15.

Surfaces of the other through-cracks from Failure 2 showed differing mixtures of corrosion and mechanical fracture. For example, two of the cracks showed fairly straight surface profiles near the presumed origin on the pipe inner surfaces, and distinctly corroded profiles at greater depths. This points to undercutting of ligaments of sound metal by an environmentally-assisted process and subsequent mechanical separation of the undercut metal - as discussed previously for the WL through-crack shown in Fig. 8. Two of the cracks showed corroded surfaces at locations more than 3/4 through the pipe wall. The two metallographic sections not exhibiting cracks (Table 2) showed

corrosion pits at the weld toe which might have represented an early stage in the development of HL cracks.

With respect to SWC, the comments made with reference to Failure 1 are also applicable to Failure 2. That is, SWC was not involved in crack initiation and appeared only as a secondary phenomenon in association with some propagating SSC cracks. Minor amounts of SWC were most evident in the central third of the pipe wall, and were not seen remote from SSC cracks.

PIECES OF PIPE WALL

Three as-received pieces, flame-cut from the pipe wall near Failure 1, were given a magnetic particle inspection for surface cracks. None were seen in pieces 982-A-1 and 982-A-3, whereas four cracks detected in piece 982-A-2 are referred to below and listed in Table 1.

The three pieces were given a light de-scaling in inhibited hydrochloric acid. The inner surfaces were then examined, using a low-power stereomicroscope. Two of the pieces did not exhibit cracks on the mill weld faces or in the adjacent weld HAZ. However, piece 982-A-1 showed a number of apparently shallow surface cracks in parent metal on one side of the weld; one of them was underlain by a blister. The cracks lay parallel to the weld direction and were 5-12 mm from the weld over a longitudinal distance of about 75 mm. Parent metal cracks such as these did not contribute to the failure and were therefore considered to be only of academic interest.

One side of piece 982-A-2 is part of the major WL failure crack in Failure 1. A composite view of the surface of this crack, after light de-scaling, is shown in Fig. 16. The left-hand side of the fracture surface, as shown in this figure, is at what was reported to be the failure initiation zone.

The fracture surface on piece 982-A-2 did not show significant necking. There was a small, but definite, shear lip on some parts of the outer edge, indicative of final mechanical fracture, but this feature was absent from the inner edge. In an area to the left of centre of Fig. 16, the WL fracture wandered over to the weld HAZ for a short distance, and delamination in the plate rolling plane occurred. Adjacent to this is a notch where a sample has been cut out.

The locations and type of four secondary cracks identified by magnetic particle examination are shown in Fig. 16. Cracks 2 (HL) and 3 (WL-WT)

are not clearly visible, but are located at the light patches of paint, used to mark their position after detection.

The fracture surface in Fig. 16 shows a poorly defined longitudinal boundary between the inner and outer weld passes. Closely corresponding with the areas occupied by the two weld passes are:

i) an inner zone, exhibiting unusual fan-like groupings of curved ridges originating at a number of points on the weld inner face;

ii) an outer zone with a rougher surface, exhibiting approximately parallel ridges in the through-thickness direction. Under low power magnification, this zone appeared to consist of metal torn in the through-thickness direction.

Figure 17 shows one of the fan-like groupings of ridges on the major WL fracture surface, at secondary crack 1 (WT). There is a difference in appearance between the inner and outer crack zones, noted above.

The major WL fracture surface was examined across the pipe wall thickness, by scanning electron microscope at high magnification, for a longitudinal distance of about 20 mm, centering on crack 1 (WT). All fracture surfaces were found to be dimpled, indicating that fracture had occurred by microvoid coalescence. Figure 18 shows a typical view in the area examined.

Part of secondary crack 1 (WT) was opened out for examination of its surfaces by scanning electron microscope. Figure 19 shows the two matching halves of the area examined, whose lengths represent about half the depth of crack 1 (WT). As shown in Fig. 20, fracture surfaces of the secondary crack were found to be dimpled, resembling those of the major WL failure crack. A number of tertiary micro-cracks were observed on the surfaces of secondary crack 1 (WT), and one of these is shown in Fig. 21.

HARDNESS MEASUREMENTS

Rockwell hardness measurements were made on five typical metallographic sections from Failures 1 and 2. Figures 22-26 show relevant microstructure boundaries and cracks schematically. The Rockwell hardness measurements were made at locations marked on the figures by a cross; circled crosses in the associated graph indicate the hardness values obtained. These results also appear in Table 3, along with Rockwell hardness values obtained in measurements on weld specimens, cut transverse to the weld bead, from pieces 982-A-1, 982-A-2 and 982-A-3.

Tukon microhardness measurements were also performed, mainly to indicate differences in hardness of different microstructures. A conversion chart in use at PMRL was corrected to give converted Rockwell hardnesses on the basis of numerous Tukon-Rockwell comparisons made by the writers at HRB 90, and at HRC 25. In Fig. 22-25, the locations of Tukon microhardness measurements are shown by short vertical lines, and the converted Rockwell values by circled points on the associated graph.

The dark, oval ring observed near the origin of the WT crack, shown in Fig. 10, was found to exhibit much higher converted Rockwell hardness values than the remainder of the weld. This is shown in Fig. 25.

There was no indication of hardening in the coarse-grained HAZ, in which all HL cracks initiated. Slight softening was observed in the fine-grained HAZ.

DISCUSSION OF RESULTS

Condensate must have been present for at least part of the time in the failed part of the H_2S-containing Grizzly Pipeline, because the pipe inner surfaces were corroded and scaled. With the tensile stress deriving from operating pressure and residual stresses from pipe fabrication, the prerequisites for SSC were fulfilled.

Crack profiles from the Grizzly Pipeline failure resembled the very few examples of SSC, obtained in laboratory tests on relatively soft steels (2,4,7,9). An example of SSC in a line-pipe steel, observed in research at PMRL, appears in Fig. 27 (10).

METALLOGRAPHY

Examination of the mounted metallographic sections from the Grizzly Pipeline indicated there were two types of crack surface:

i) Corroded (SSC), showing such features as shallow pits, corrosion film, micro-cracks and irregular, indented surface profiles;

ii) Mechanically fractured, showing distorted microstructure and metal, little or no corrosion, and generally flat or smoothly curved surface profiles.

Cracks partly through the pipe wall showed corroded surfaces only, which is consistent with the initiation and propagation of SSC cracks, and

the continuing corrosion of crack surfaces by the H_2S-containing environment. On the other hand, cracks which had penetrated through the pipe wall always showed both mechanically fractured and corroded surfaces.

These observations indicate that sulphide stress-cracks initiated inside the pipe, on the weld face and in the weld HAZ. The cracks propagated generally in the through-thickness direction, sometimes by-passing and undercutting ligaments of sound metal. When the SSC progressed to such an extent that the remaining sound metal was unable to tolerate the applied tensile stresses, mechanical fracture occurred.

FRACTOGRAPHY

Fractographic examinations were all performed on a major WL fracture surface of Failure 1. Results were consistent with conclusions from the metallographic examinations; Fig. 16 and 17 show that there are inner and outer zones which can be attributed respectively to SSC and mechanical fracture. In the inner zone, each of the unusual fan-like groupings of ridges may represent an individual SSC initiation. After SSC penetrates about halfway through the pipe wall, the remaining sound metal cannot withstand the operating stresses (plus possible residual tensile stresses), and fails by mechanical fracture. Examinations across the major WL fracture surfaces, with a scanning electron microscope at high magnification, failed to differentiate between the two zones assumed to represent SSC and mechanical fracture. Dimpling (microvoid coalescence) was observed in both cases and also on the surfaces of secondary weld crack 1 (WT).

Dimpling is often taken as indicative of a failure by mechanical overload. However, as applied to the entire fracture surface this interpretation cannot be sustained, especially in view of the metallographic evidence. It is more reasonable to accept C.D. Beachem's demonstration that dimpled surfaces can be produced by hydrogen-assisted processes, such as SSC, as well as by mechanical failure (11).

HARDNESS MEASUREMENTS

Rockwell hardness determinations on pipe samples from Failures 1 and 2 gave values of HRB 83-96 for the weld, weld HAZ, and parent metal. The average hardness was HRB 90 (HRC 9). This is well below the maximum of HRC 22 specified by the National Association of Corrosion Engineers (NACE) to

minimize SSC in sour service (12) - a specification supported by considerable service experience (3).

However, many laboratory tests carried out by the writers have shown SSC in steels with hardness well below HRC 22 (2,3). It appears that a normally acceptable steel in a sour-gas pipeline, even though its hardness is below HRC 22, may fail by SSC if the stress and environmental conditions are severe enough.

Absolute values of converted Rockwell hardnesses from Tukon microhardness determinations are generally considered questionable; but at least, they are indicative of differences in hardness in and near the weld. Relative to parent metal, Fig. 22, 23, 24, and 26 show some softening in the fine-grained HAZ. Neither hardening nor softening were evident in the coarse-grained HAZ, in which HL sulphide stress cracks initiated.

As shown in Fig. 25, the Tukon microhardness measurements indicated that a 2.5 mm long, dark, oval ring at a weld face near Failure 1 was a hard spot, with converted Rockwell hardness readings of HRC 26-32.

Using the electron probe microanalyser, alloy composition was determined beside each of the Tukon indentations designated in Fig. 25. The results appear in Table 4 and show that hard areas were significantly enriched in Mn and Si (13).

The Mn and Si probably originated in the slag in the submerged-arc welding process, but their appearance as a segregate in the metal, rather than as a Mn-Si oxide inclusion, seems unusual. In the hard areas, the steel microstructure had the appearance of martensite, which would be consistent with a Mn content of over 3% (14).

Only the above hard spot was detected, but it is conceivable others were present. However, in view of the extensive HL cracking in the Grizzly Pipeline, weld hard spots cannot explain the failures and there was nothing to indicate that they played a significant role.

OTHER CRACKING MECHANISMS

While it was concluded that SSC was the primary cause of the Grizzly Pipeline failures, other cracking mechanisms which were considered are discussed briefly below.

(1) Stepwise Cracking (SWC)

SWC is a type of H_2S-induced cracking which occurs in parent and weld HAZ but not in the weld fusion metal. SWC develops primarily at inclusions and propagates most readily in the rolling plane of the steel, however, transverse cracks can appear, imparting a step-like appearance. SWC can occur in steels which are not externally stressed and in steels under tensile stress (5).

Because weld metal is immune to SWC, WL and WT sulphide stress cracks observed in the Grizzly Pipeline cannot be attributed to this mechanism. HL sulphide stress-cracks initiated in the coarse-grained HAZ, and there was no indication that SWC was involved in their initiation. However, when a sulphide stress-crack propagated into the fine-grained HAZ or the edge of the parent metal, minor amounts of SWC were sometimes seen in the main crack in the form of abrupt bends and short branches in the rolling plane. There were also a few small SWC groups at a short distance from the crack. These manifestations were mostly limited to the central third of the wall thickness, and SWC remote from sulphide stress-cracks was not observed. In summary, SWC was considered a purely secondary phenomenon which did not contribute significantly to the Grizzly Pipeline failure.

(2) Corrosion Fatigue

It is understood that in gas transmission pipeline service, pressure fluctuations are insufficient for corrosion fatigue to be considered seriously as a failure mechanism. Furthermore, the cracking in the Grizzly Pipeline showed the following characteristics which were inconsistent with corrosion fatigue:

i) Cracks often initiated on the weld faces, rather than in the obvious stress raiser at the edge (toe) of the weld, where fatigue or corrosion fatigue cracks would be expected to initiate.

ii) In the large WL fracture face in Failure 1, the SSC zone was rougher than would be expected in a fatigue crack, and the fan-like groupings of curved ridges differed from the "beachmark" morphology often seen in fatigue.

iii) The mixture of longitudinal and transverse cracks seen in the Grizzly Pipeline contrasts with the systems of fairly straight, parallel cracks often observed in corrosion fatigue.

It is concluded that corrosion fatigue did not play a part in the pipeline failures.

(3) Weld Cold Cracking

Weld cold cracking (WCC) is caused by hydrogen diffusing from a newly-produced weld into susceptible structures. WCC can produce a number of different crack types, including those (WT, WL, HL) seen in the Grizzly Pipeline and under-bead and root-cracking as well. However, in the low-hydrogen, high heat input, submerged-arc welding process used in manufacture of the pipe, there is very little likelihood of WCC in mill welds. In addition, if there were any WCC, it would be more likely to occur in a second weld pass because the first pass is heated for a longer period, facilitating the loss of hydrogen (14). But the Grizzly Pipeline cracking initiated entirely in the first (inner) weld pass, or in the adjacent HAZ. This behaviour is inconsistent with WCC, and is further evidence that it did not contribute to the pipeline failures.

CONCLUSIONS

The National Energy Board supplied samples of damaged line-pipe from the July 1981 failures of the Grizzly sour-gas pipeline. These have been examined and the following conclusions were made regarding the failure mechanisms:

1. The cause of the failures was the development of sulphide stress cracking (SSC) in the weld and weld HAZ, originating on the inside of the line-pipe.
2. The SSC propagated through the pipe wall to a depth sufficient for the operating (plus any residual) tensile stresses to cause rupture of the pipe by mechanical overload.
3. Stepwise cracking (SWC) was observed in connection with some of the SSC in the weld HAZ, but was considered to be a secondary phenomenon, not contributing to the pipeline failures.
4. Corrosion fatigue and weld cold cracking did not contribute to the pipeline failures.

5. Rockwell hardness measurements on the pipe weld, weld HAZ and parent metal averaged about HRB 90 (HRC 9), i.e., well below the maximum hardness of HRC 22 specified by the National Association of Corrosion Engineers to minimize SSC in sour service. There was no hardening in the weld HAZ. Tukon microhardness measurements revealed one weld hard spot (HRC 26-32) but this was not considered to contribute significantly to the failures.

ACKNOWLEDGEMENTS

Useful discussions were conducted with J.B. Gilmour, R.W. Revie, O. Vosikovsky and J.T. McGrath of PMRL, CANMET, EMR. PMRL Photographic and Draughting Services provided valuable assistance, and V.E. Moore of Engineering and Metal Physics Section, PMRL, performed measurements using the electron probe microanalyser. V.P. Chartrand of the same section provided assistance with measurements using the scanning electron microscope. D. Lusk of the Nondestructive Testing Section, PMRL, performed magnetic particle examinations on pipe specimens. D.W.G. White and C. Champion performed a thorough editorial scrutiny of this report.

REFERENCES

1. Erickson, W.H., Director; PMRL, CANMET, EMR; Letter to Eickmeier, J.R. , Director, Gas Pipelines Group, National Energy Board, Ottawa, February 5, 1982.

2. Tuttle, R.N. and Kane, R.D., editors, "H_2S corrosion in oil and gas production - a compilation of classic papers"; Houston, National Association of Corrosion Engineers; 1981.

3. Carter, C.S. and Hyatt, M.V. "Review of stress-corrosion cracking in low-alloy and low-strength steels"; Int Conf Stress-corrosion Cracking and Hydrogen Embrittlement of Iron-base Alloys; June 10-16, 1973; Unieux-Firminy, France; 1974.

4. Greer, J.B. "Factors affecting the sulphide stress cracking performance of high strength steels"; Mater Perform 14:3:11-22; 1975.

5. Biefer, G.J. "Factors affecting the stepwise cracking of line-pipe steels in sour environments"; Division Report ERP/PMRL 81-5 (J); CANMET, Energy, Mines and Resources Canada; 1981.

6. Nakashima, A., Iino, M., Matsuda, H. and Yamada, K. "Stepwise cracking of pipelines"; Paper 30.3 Proc 20th Ann Conf Metallurgists CIM; Aug. 23-27, 1981; Hamilton; 1-32; 1981.

7. Taira, T. and Kobayashi, Y. "Full size SSC test result of line pipe under wet sour gas environments"; Paper 183 Corrosion 81; April 6-10, 1981; Toronto; 183/1 - 183/18; 1981.

8. Herbsleb, G., Poepperling, R.K. and Schwenk, W. "Occurrence and prevention of hydrogen-induced stepwise cracking and stress corrosion cracking of low alloy pipeline steels"; Corrosion-NACE 36:5:247-256; 1981.

9. Taira, T., Tsukada, K., Kobayashi, Y. Inagaki, H. and Watanabe, T. "Sulphide corrosion cracking of line pipe for sour gas service"; Corrosion-NACE 37:1:5-16; 1981.

10. Revie, R.W. and Fichera, M. "Unpublished data"; PMRL, CANMET, Energy, Mines and Resources Canada; Ottawa, 1979.

11. Beachem, C.D. "A new model for hydrogen-assisted cracking (hydrogen "embrittlement")"; Metall Trans 3:2:437-451; 1972.

12. National Association of Corrosion Engineers; "Material Requirement: Sulphide stress cracking resistant material for oil field equipment"; NACE Standard MR-01-75 (1980 Revision); 1980.

13. Moore, V.E., Private Communication; PMRL, CANMET, Energy, Mines and Resources Canada; Ottawa, 1982.

14. McGrath, J.T., Private Communication; PMRL, CANMET, Energy, Mines and Resources Canada; Ottawa, 1982.

Table 1. Number and type of major cracks observed in as-received samples of pipe taken at Failure 1 (982)

Pipe section						
A-1	Section M-2: No cracks	Piece A-1 No cracks (MP)				
A-2	Section M-14 3 WL cracks	Section M-15 No cracks	Piece A-2 1 WT, 1 HL 1 HL-WL 1 WL-WT (MP)			
A-3	Section M-4: No cracks	Section M-5 1 WT crack	Section M-6 1 HL crack	Section M-7 1 WL crack	Section M-20 1 WT crack	Piece A-3 No cracks (MP)
B	Section M-9 1 HL crack	Section M-11 1 WL crack	Section M-19 2 WL cracks			

Crack description: HL - in weld HAZ, parallel to weld; MP = magnetic particle inspection.
WL - in weld, running along its length;
WT - in weld, transverse to its length.

Table 2. Number and type of major cracks observed in as-received metallographic sections taken at Failure 2 (1004)

Pipe section					
A-1	Section M-1 No cracks	Section M-2 No cracks			
A-2	Section M-3 1 HL crack	Section M-4 1 HL crack	Section M-8 1 HL crack	Section M-9 1 HL crack	Section M-10 1 WL crack

Crack description: HL - in weld HAZ, parallel to weld;
WL - in weld, running along its length.

Table 3. Rockwell hardness determinations on steel samples from failed pipes

Source	Type	Hardness, Rockwell B			
		Number	Parent	HAZ	Weld
Failure 1	Received as metallo graphic section	982-M5	-	-	90,93,90
"	"	982-M9	88,92,92	-	92
"	"	982-M11	88,89,89	-	92
"	"	982-M14	86,91,92	-	93
Failure 2	"	1004-M8	92,92,90	-	92
Failure 1, flame cut pieces	Metallographic sections cut from pieces.	982-A-1-W	86,88	83	83,84,90
"	"	982-A-2-W	91,93	89	94,96,90
"	"	982-A-3-W	88	87	90,88
		Av	90	86	90

Table 4. Weight percent of elements obtained by electron probe measurements at different locations near hard spot in weld (13)

Location*	Cr	Mn	Fe	Ni	Cu	Si	Total	Hardness,** Rockwell
1	0.069	2.281	98.078	0.017	0.151	0.225	100.820	HRB 96
2	0.055	3.247	96.105	0.118	0.197	1.074	100.797	HRC 32
3	0.049	2.097	98.552	0.113	0.210	0.186	101.207	HRB 95
4	0.043	2.713	96.959	0.094	0.197	0.451	100.458	HRC 26
5	0.044	3.579	97.343	0.099	0.153	1.177	102.395	HRC 27
6	0.028	2.275	96.611	0.046	0.178	0.215	99.354	HRB 96
A	0.039	2.049	95.144	0.082	0.150	0.214	97.678	HRB 96
B	0.033	2.099	94.530	0.117	0.155	0.182	97.116	HRB 95
C	0.029	2.046	95.501	0.090	0.173	0.168	98.007	HRB 93
D	0.028	2.284	95.073	0.067	0.213	0.197	97.861	HRB 92
E	0.065	2.203	94.699	0.046	0.171	0.234	97.417	HRB 91
F	0.041	1.940	95.361	0.032	0.138	0.209	97.720	HRB 95
G	0.070	2.107	95.433	0.143	0.121	0.192	98.065	HRB 94

*See Fig. 25

**As converted from Tukon microhardness measurements

Fig. 1. (Failure 1, 982-A-1) Inside surfaces of as-received piece flame-cut from pipe section A-1. ~X0.5 (neg 5843)

Fig. 2. (Failure 1, 982-A-2) Inside surfaces of as-received piece flame-cut from pipe section A-2. The lower side is a major WL fracture surface on the failed pipeline, and the failure initiation zone is at the right hand side of the photograph. ~X0.5 (neg 5839)

Fig. 3. (Failure 1, 982-A-3). Inside surfaces of as-received piece flame-cut from pipe section A-3. ~X0.5 (neg 5840)

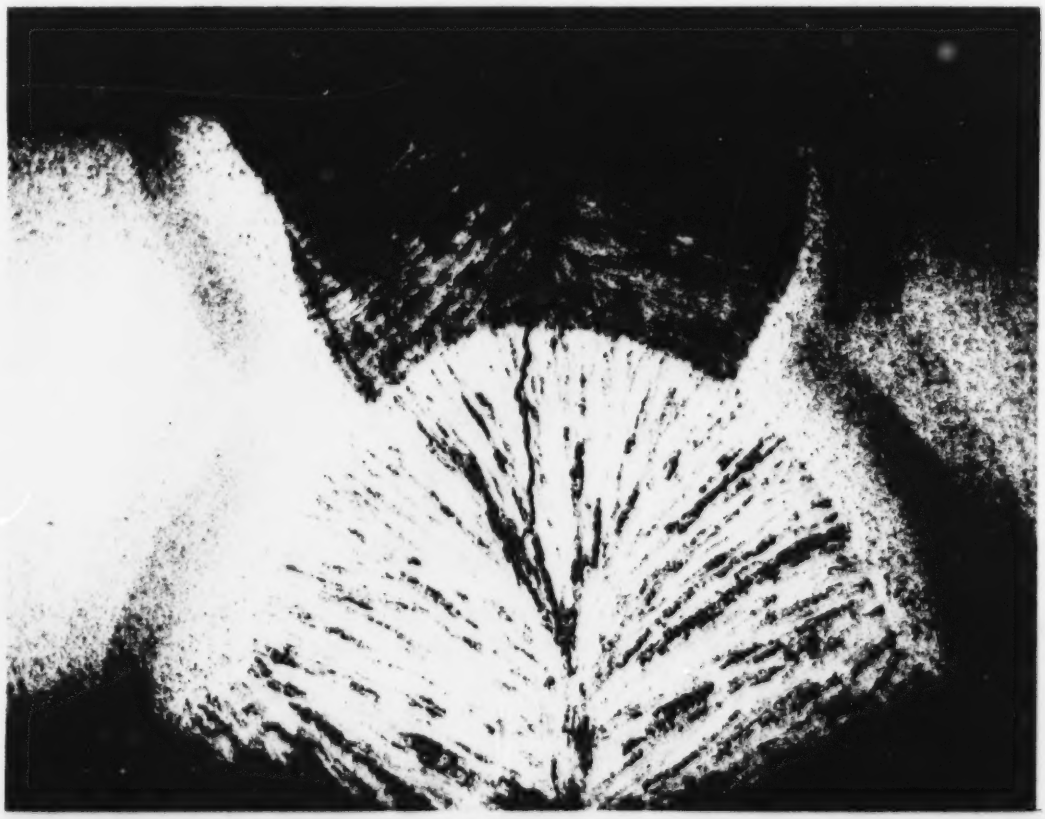

Fig. 4. (Failure 1, 982-M11). WL crack in pipe section B. X9.5 (neg 6290)

Fig. 5. (Failure 1, 982-M11) Corroded appearance of WL crack in pipe section B, near crack origin. X100 (neg 6291)

Fig. 6. (Failure 1, 982-M9) HL crack in pipe section B. X20 (neg 6292)

Fig. 7. (Failure 1, 982-M9) Tip of HL crack in pipe section B. X100 (neg 6293)

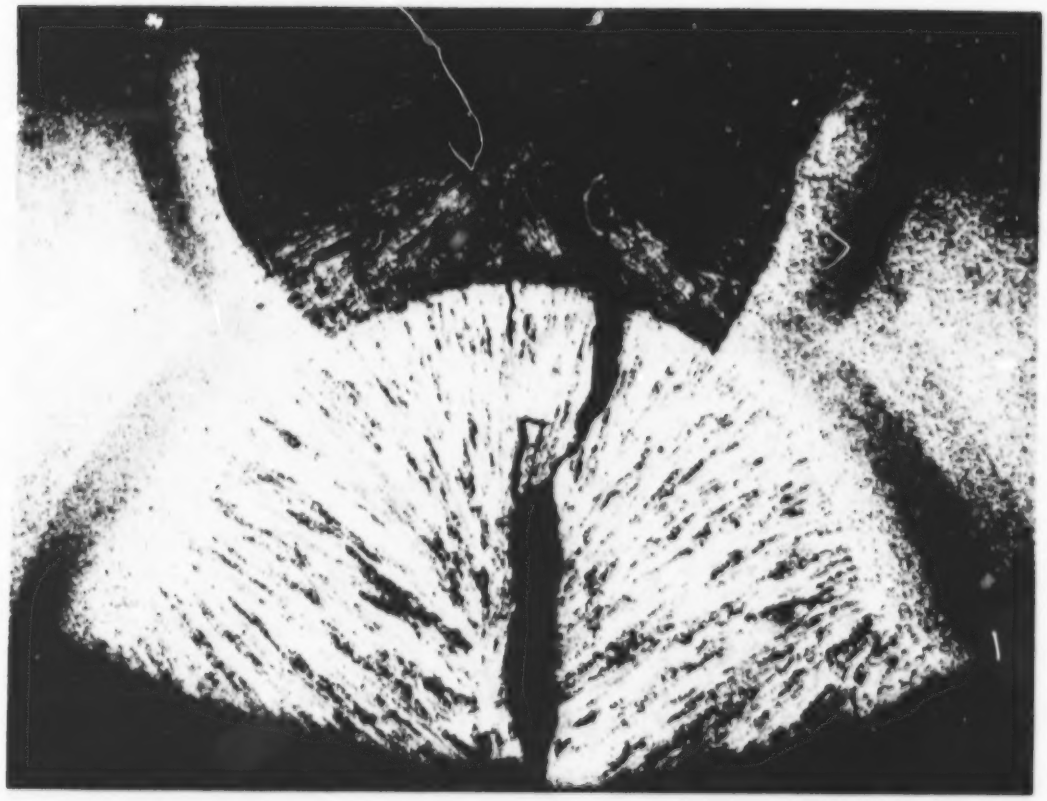

Fig. 8. (Failure 1, 982-M14) Multiple WL cracks in pipe section A2, near the pipe failure initiation zone. X9.5 (neg 6294)

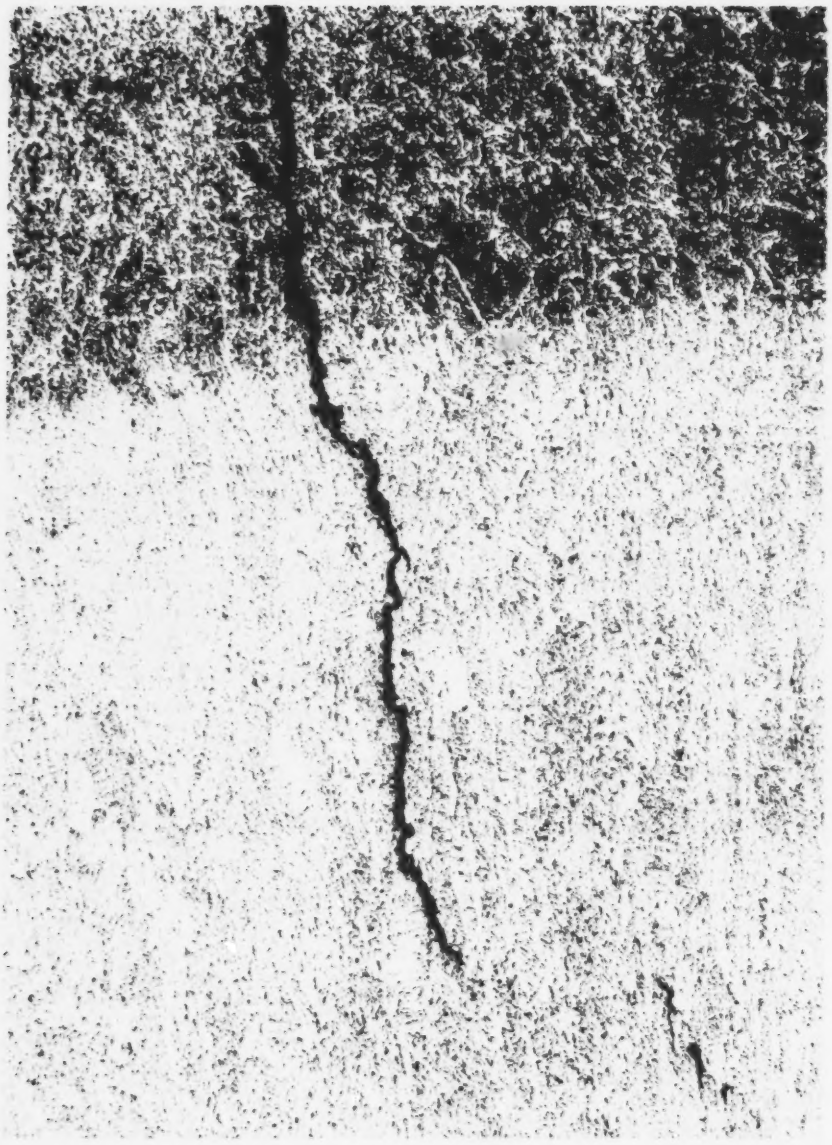

Fig. 9. (Failure 1, 982-M14) Tip of WL crack in pipe section A-2. The first (inner) weld pass is at the top of the photograph. X100 (neg 6295)

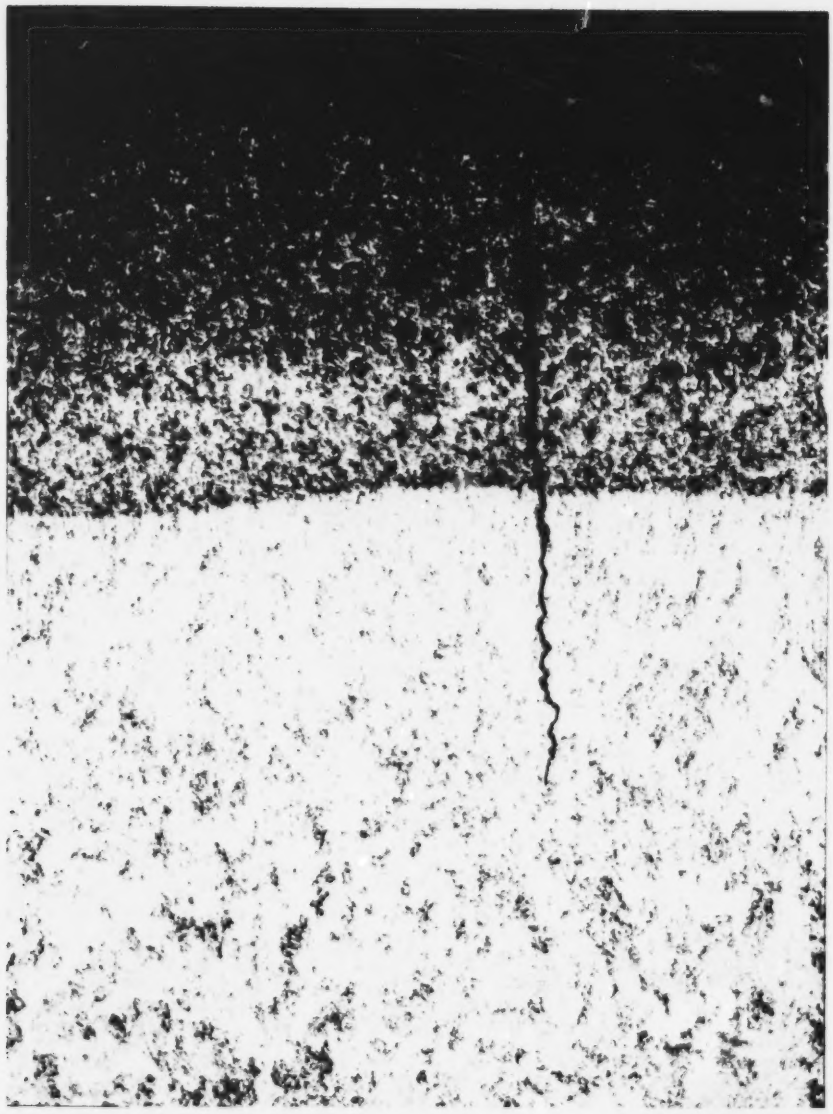

Fig. 10. (Failure 1, 982-M5) WT crack in longitudinal section of weld in pipe section A-3; the dark, oval ring near the crack origin is a hard spot. X13.25 (neg 6296)

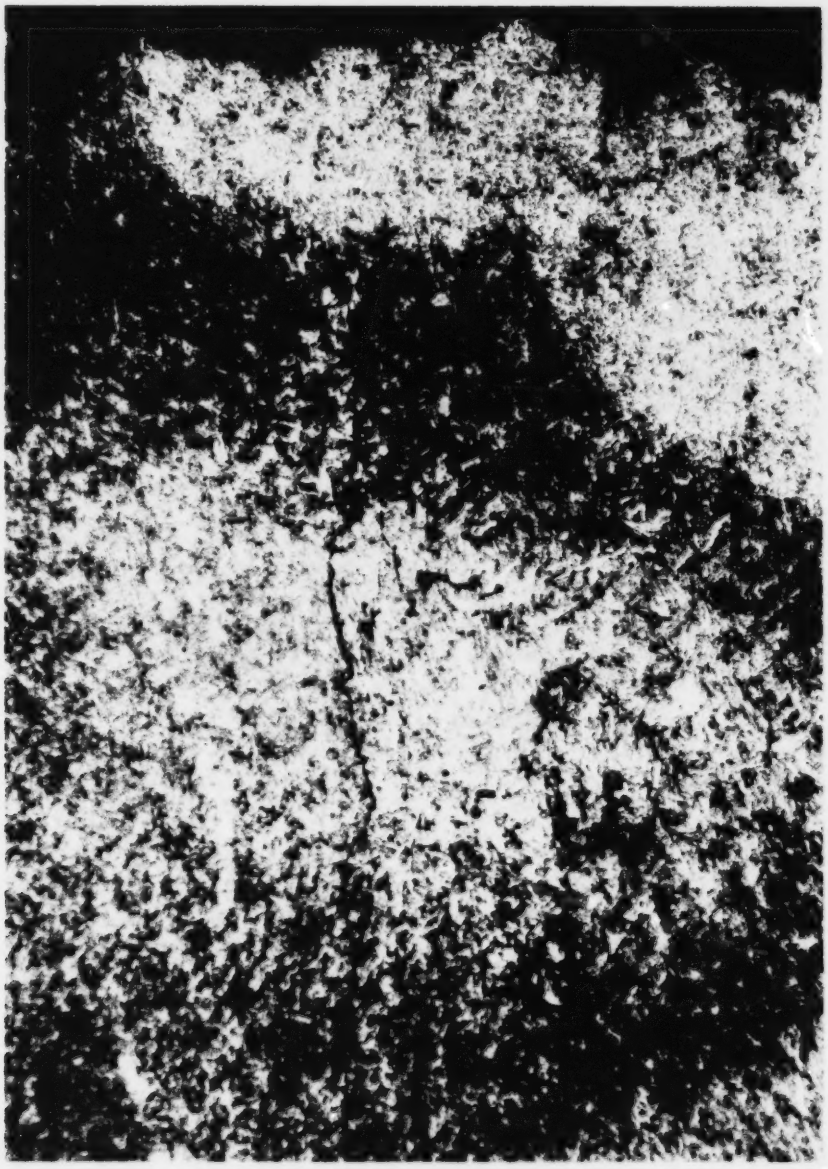

Fig. 11. (Failure 1, 982-M5) Microcrack within hard spot in longitudinal section of weld in pipe section A-3. X300 (neg 6297)

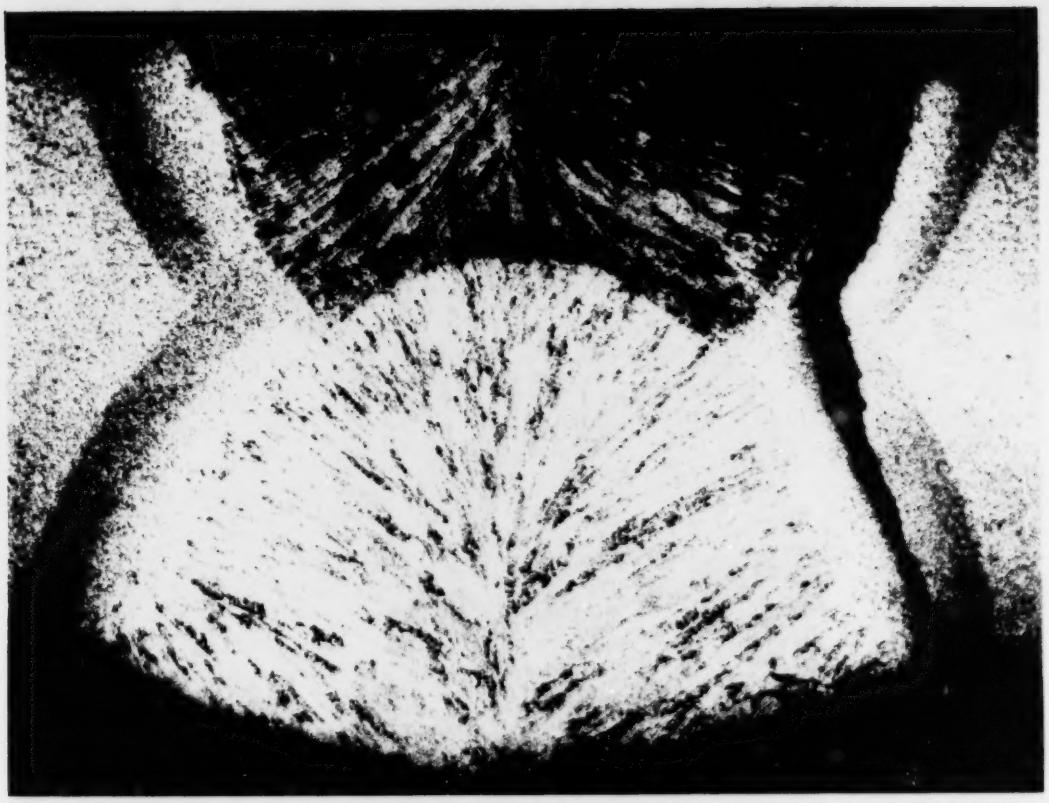

Fig. 12. (Failure 2, 1004-M8) Through-thickness HL crack in pipe section A-2. X9.6 (neg 6298)

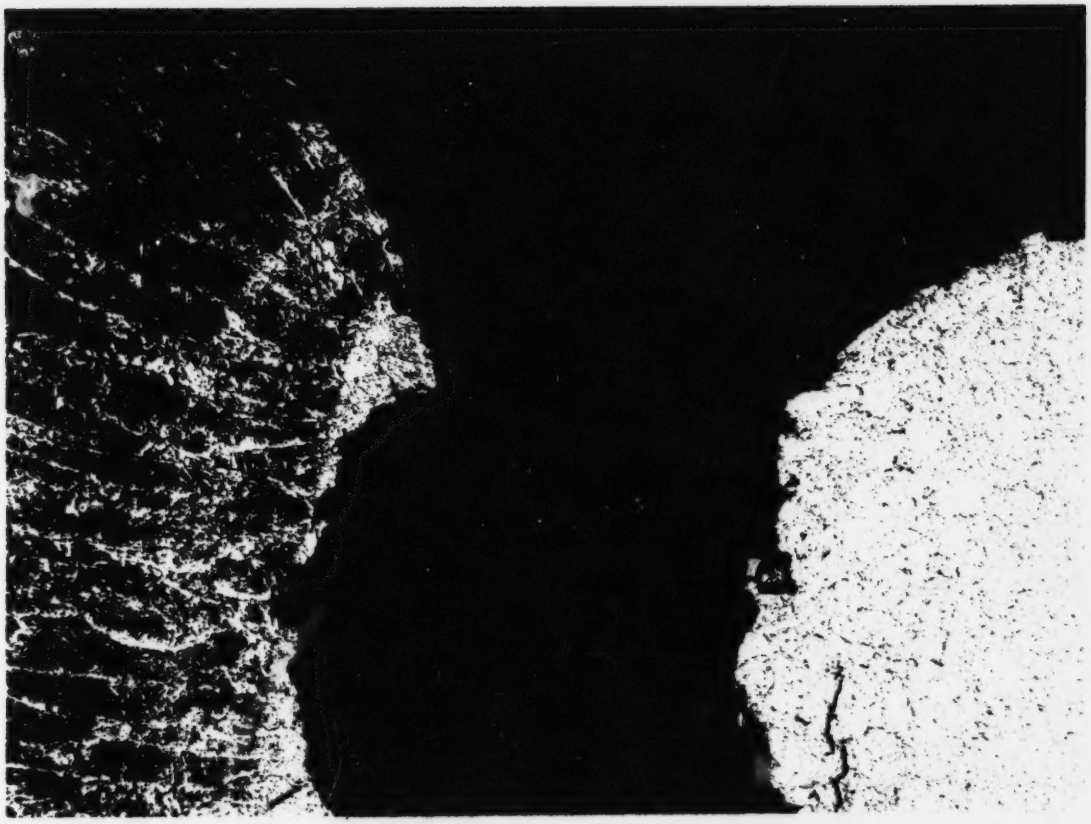

Fig. 13. (Failure 2, 1004-M8) Origin of through-thickness HL crack in pipe section A-2. X100 (neg 6299)

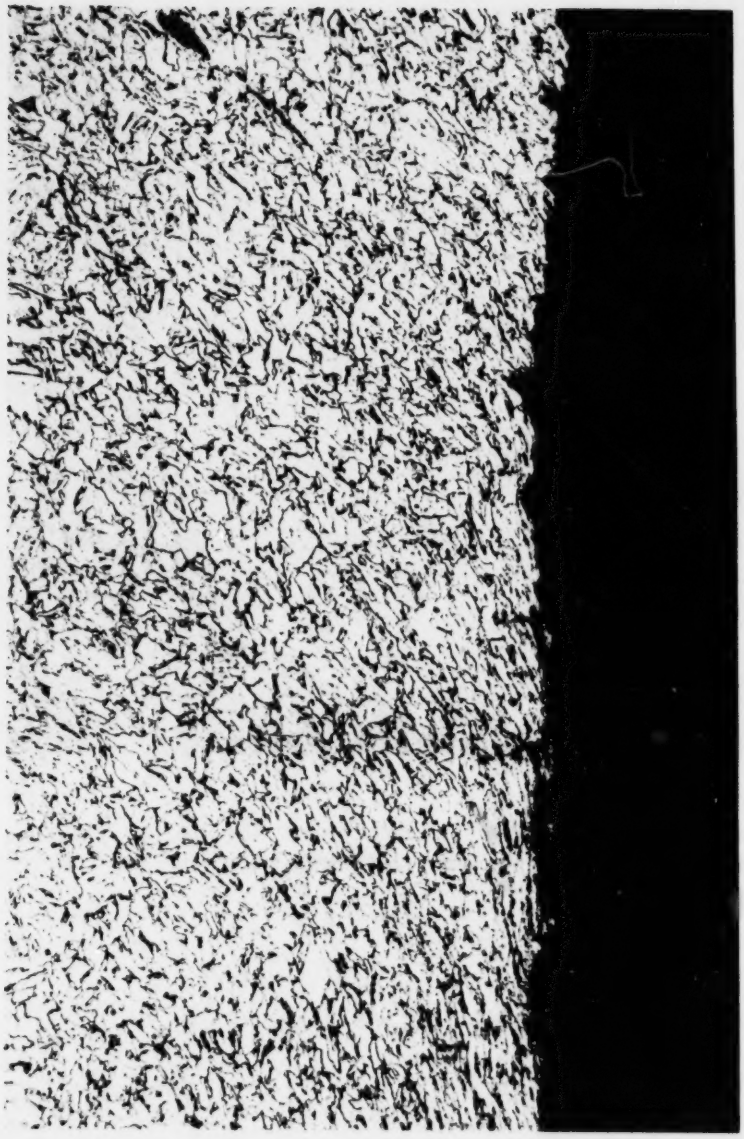

Fig. 14. (Failure 2, 1004-M8) Section of through-thickness HL crack in pipe section A-2 at a point about halfway through pipe wall, showing deformed microstructure at crack surface in weld HAZ. X300 (neg 6300)

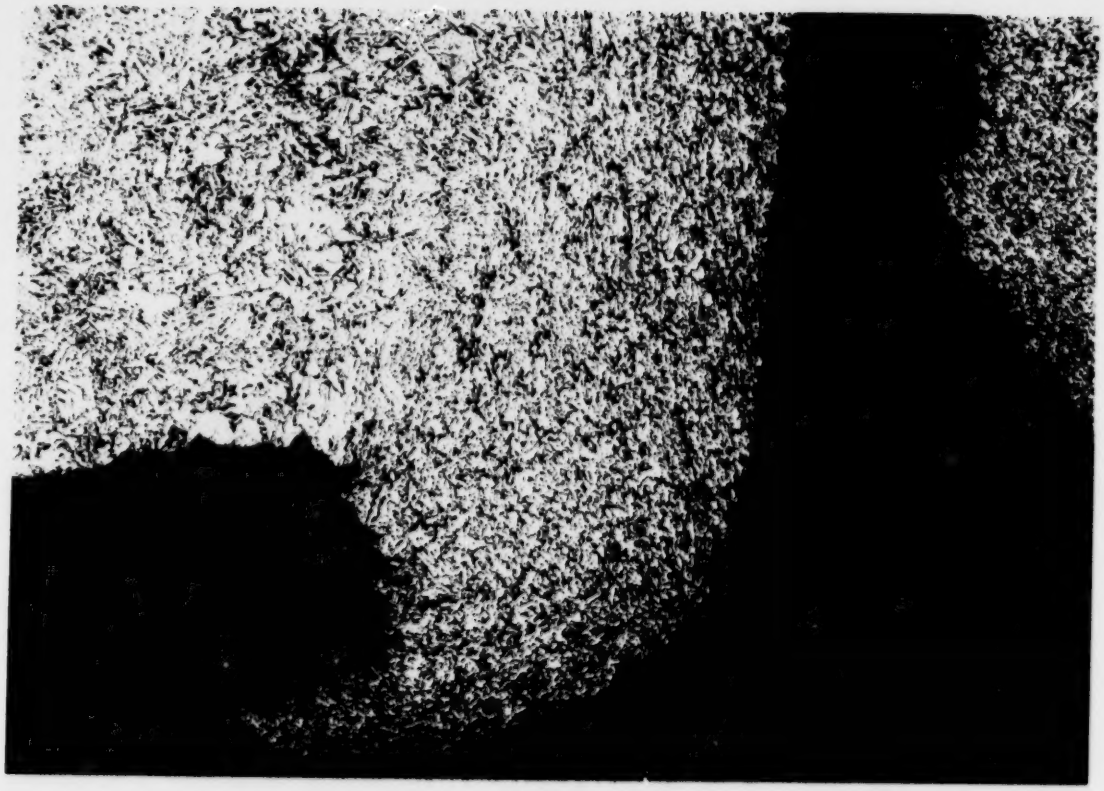

Fig. 15. (Failure 2, 1004-M8) Termination of through-thickness HL crack in pipe section A-2, showing deformed metal in weld HAZ. X100 (neg 6301)

ig. 16. Major WL fracture surface on piece 982-A-2, pipe section A-2 of failure 1. X1. (neg 6283)

Fig. 17. (Failure 1, piece 982-A-2) SEM photograph of secondary crack 1 (WT) on major WL fracture surface. X17.6 (neg 6284)

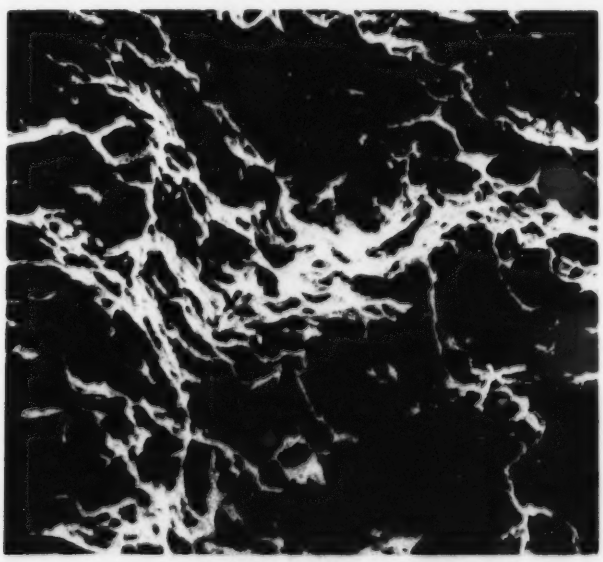

Fig. 18. (Failure 1, piece 982-A-2) SEM photograph of typical surfaces on major WL fracture near secondary crack 1 (WT). X1870 (neg 6279)

Fig. 19. (Failure 1, piece 982-A-2) SEM photograph of fracture surfaces of secondary crack 1 (WT). Crack origin is along shorter side at right. X19.8 (neg 6281)

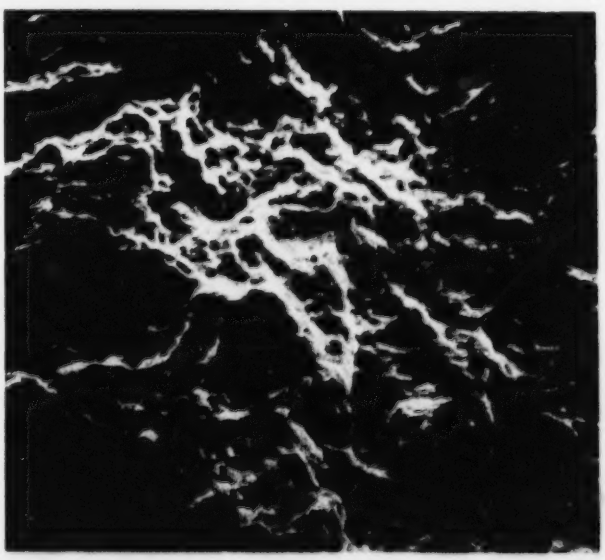

Fig. 20. (Failure 1, piece 982-A-2) SEM photograph of typical surfaces on secondary crack 1 (WT). X1980 (neg 6282)

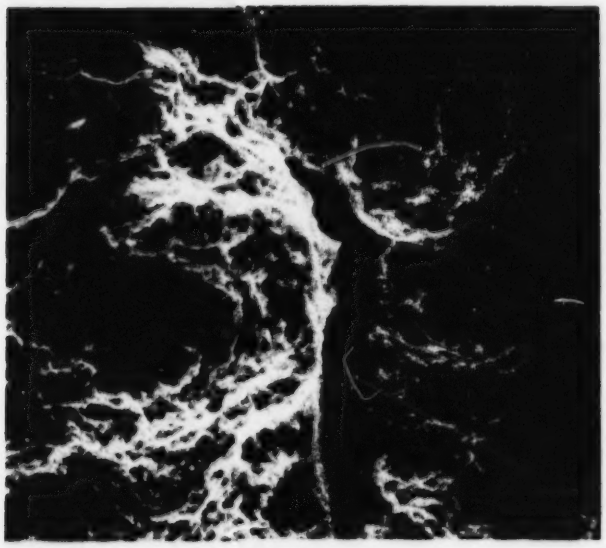

Fig. 21. (Failure 1, piece 982-A-2) SEM photograph of surfaces of secondary crack 1 (WT) showing a tertiary microcrack. X1980 (neg 6280)

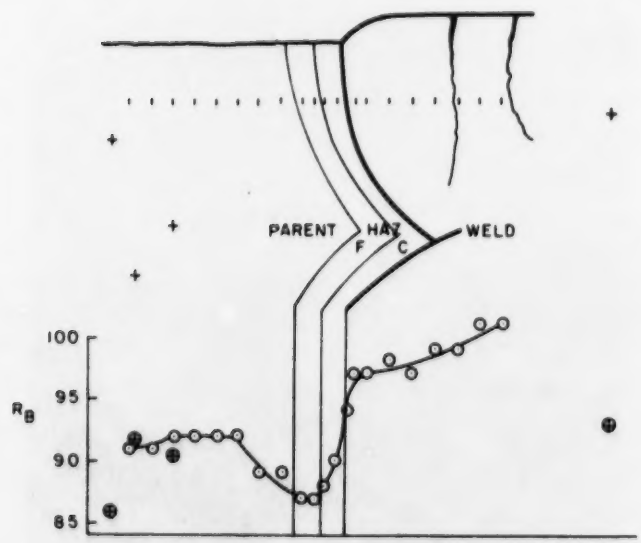

Fig. 22. (Failure 1, 982-M14) Tukon (⊙) and Rockwell (⊕) hardness determinations on section showing multiple WL cracks (cf Fig. 8). Uncircled points show locations of indentations. (neg 6288)

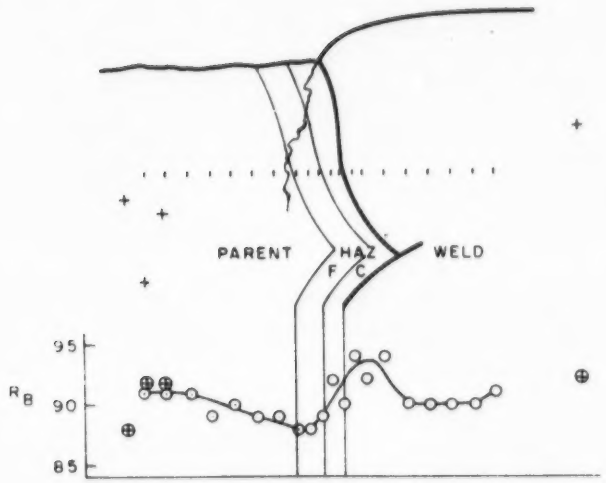

Fig. 23. (Failure 1, 982-M9) Tukon (⊙) and Rockwell (⊕) hardness determinations on section showing HL crack (cf Fig. 6). Uncircled points show locations of indentations. (neg 6287)

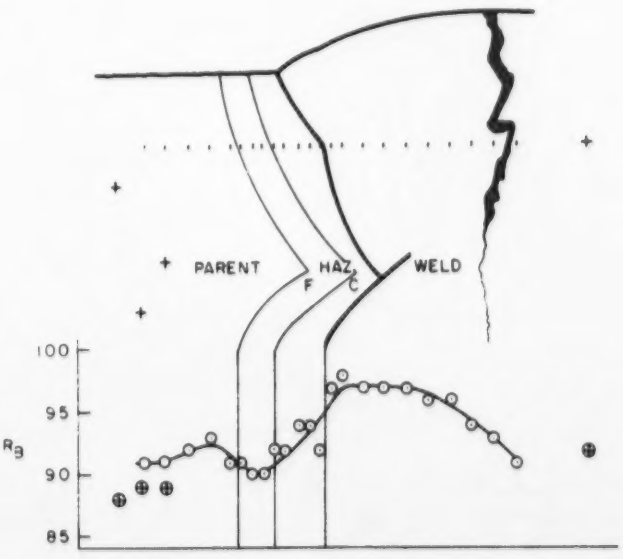

Fig. 24. (Failure 1, 982-M11) Tukon (⊙) and Rockwell (⊕) hardness determinations on section showing WL crack (cf Fig. 4). Uncircled points show locations of indentations. (neg 6286)

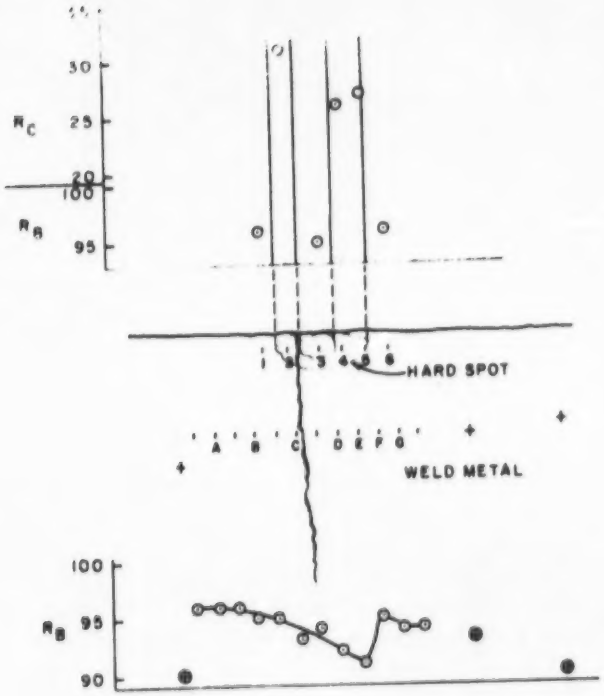

Fig. 25. (Failure 1, 982-M5) Tukon (⊙) and Rockwell (⊕) hardness determinations in longitudinal section showing WT crack and hard spot (cf Fig. 10). Uncircled points show locations of indentations. (neg 6289).

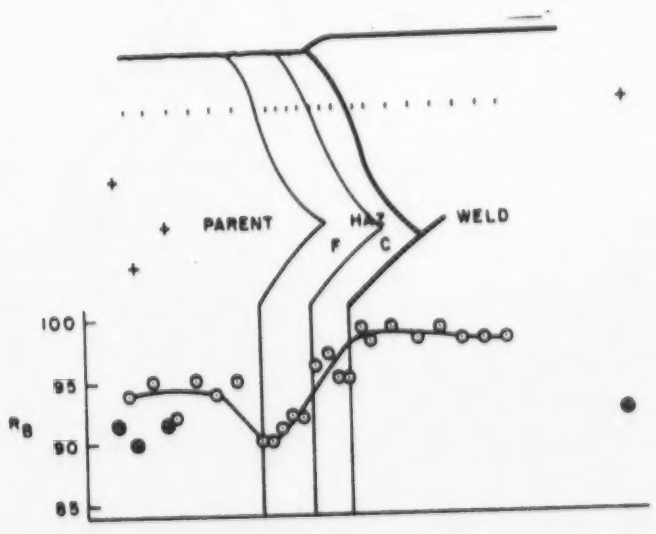

Fig. 26. (Failure 2, 1004-M8) Tukon (⊙) and Rockwell (⊕) hardness determinations on section showing HL through-crack (cf Fig. 12). Uncircled points show locations of indentations. (neg 6285)

Fig. 27. Sulphide stress cracking in laboratory test on U-bend weld specimen of Grade 483 line-pipe steel in H_2S environment (10). X40 (neg 6302)

APPENDIX I

NATIONAL ENERGY BOARD
OTTAWA, ONTARIO
K1A 0E5

CANADA

OFFICE NATIONAL DE L'ÉNERGIE
OTTAWA, ONTARIO
K1A 0E5

File No.: 1595-W5

November 9, 1981

Dr. W.H. Erikson,
Chief,
Physical Metallurgy Research Laboratories,
Department of Energy, Mines and Resources,
568 Booth Street,
Ottawa, Ontario
K1A 0E4

Dear Dr. Erikson:

RE: Request for Examination of Samples Removed from Westcoast's Grizzly Pipeline Following Two Failures in July, 1981.

Physical Metallurgy Research Laboratories is requested to conduct an investigation into the metallurgical aspects and causes of two recent failures of the Grizzly sour gas pipeline in British Columbia. We would require a report describing the results in terms of microstructure, mechanisms of crack formation, and reasons for the failures. Samples which were removed from the pipeline following the breaks in July of this year will be forwarded directly to PMRL.

The samples include mounted metallographic specimens from both the first and second failures. These are numbered as follows:

1) First failure - Specimens M2, M4, M5, M6, M7, M9, M11, M14, M15, M19, M20.

2) Second failure - Specimens M1, M2, M3, M4, M8, M9, M10.

A summary of the two failures and of previous findings are attached and the exact locations of these specimens are shown in the attachment. In addition, three coupons from the first failure will be forwarded to the laboratories. The locations of these are also described in the attachment and may be used for preparation of additional samples if required. All samples should be returned to the Board after completion of this investigation.

.../2

We request than an interim report be prepared describing the observations and findings of the examinations and a summary of probable causes of the failure as soon as is convenient. Should you require further information, please contact Dr. F. Jeglic or Mrs. B. Kenny at 996-0271.

Thank you for your cooperation.

Yours very truly,

J.R. Eickmeier
Director
Gas Pipelines Group

attach.

APPENDIX II

Summary of Information on the Grizzly Pipeline Breaks

The Grizzly Valley pipeline was constructed between January and August 1978, by Westcoast Transmission Company Limited. The line went on stream with sweet gas in December 1978 and subsequently with sour gas in February 1980. Prior to the introduction of sour gas, the line was corrosion inhibited by flood coating with Kontol and diesel fuel, vapour phase coating with Diethylamine, diesel fuel and alcohol, and the implementation of a continuous vapour phase inhibition program during service.

The typical operating pressure in sour service was between 500 and 1050 psi, and the typical gas composition from the most sour field, Bullmoose, was 0.32%N_2, 13.68%CO_2, 27.51%H_2S, 58.36%C1, 0.12% C2. The acid gas mole percentage was 41.19%, and the gas relativity density was 0.86. The gas dew point was generally below 10°F and during summer operation the gas temperature at the Bullmoose tie-in was about 60°F.

Toward the end of July, 1981, two failures occurred near the Bullmoose tie-in. The operating pressure in both cases was between 900-1000 psi at the time of failure. The pipe in question is 20 in. diameter line pipe which was fabricated from 0.375 in. wall thickness, Grade 52, (359), steel coil. This Category II, pipe (CSA Standard Z245.2) was spirally welded and supplied by Interprovincial Steel & Pipe Corporation Limited.

Following the failures, on-site investigations were conducted and pipe specimens removed. From these specimens, smaller samples of interest were removed and preliminary investigations carried out. Attached are copies of schematics showing where each sample was taken from. The designations UT and MPI refer to ultrasonic or magnetic particle indication positions.

Some general observations were as follows:

a) The fracture ran through the weld metal and the heat affected zone.

b) Magnetic particle indications generally showed cracks which ran transversely across the weld bead and longitudinally along the toe of the weld.

c) Mechanical testing revealed strengths that were some 20,000 psi higher than required by CSA Z245.2 for Grade 52 material, and notch toughness values which were acceptable but not outstanding.

d) Hardness values were generally acceptable, though high readings (above RC 22) were recorded in some regions.

.../2

Chemical analyses of the materials sampled after each failure are also attached.

Thank you for your consideration of these failures. Your help in their analysis is much appreciated.

WESTCOAST 20" GRIZZLY LINE
E81-7-982 (1ST FAILURE)

(Failure No. 1, July 20)

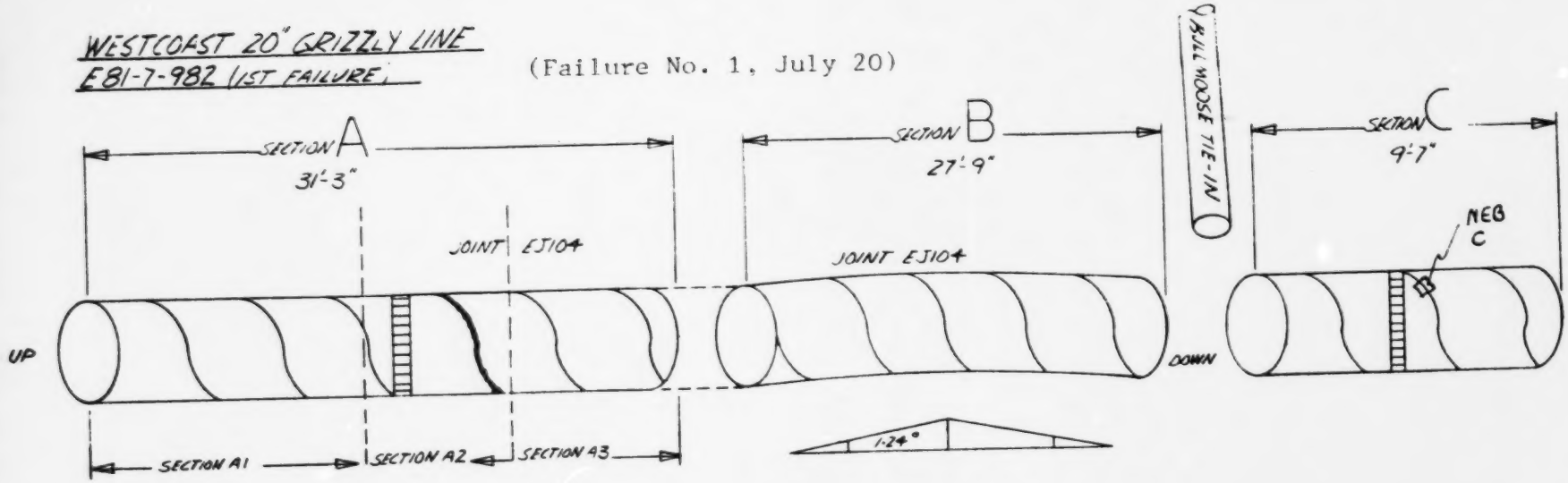

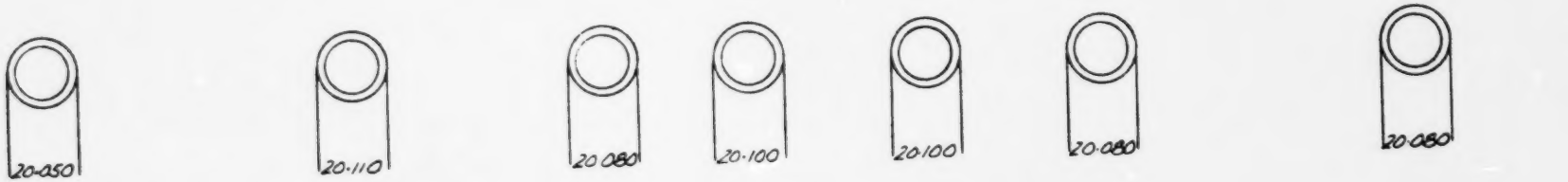

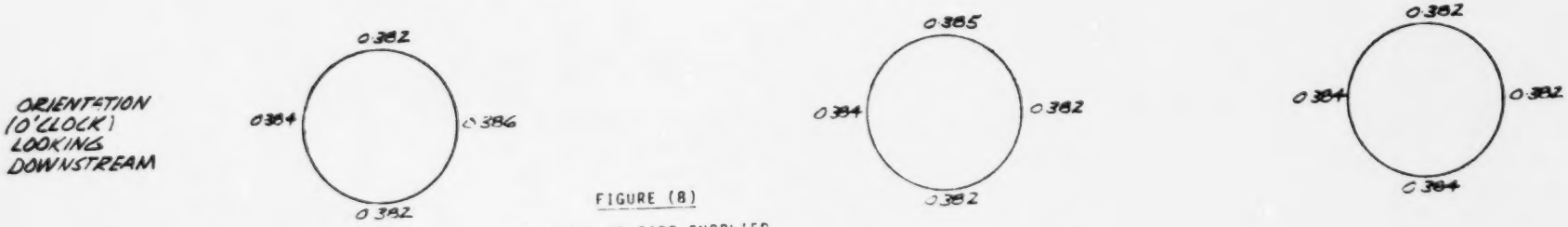

FIGURE (8)

SECTIONS OF PIPE SUPPLIED.

PIPE A SECTION A1 (Failure No. 1, July 20)

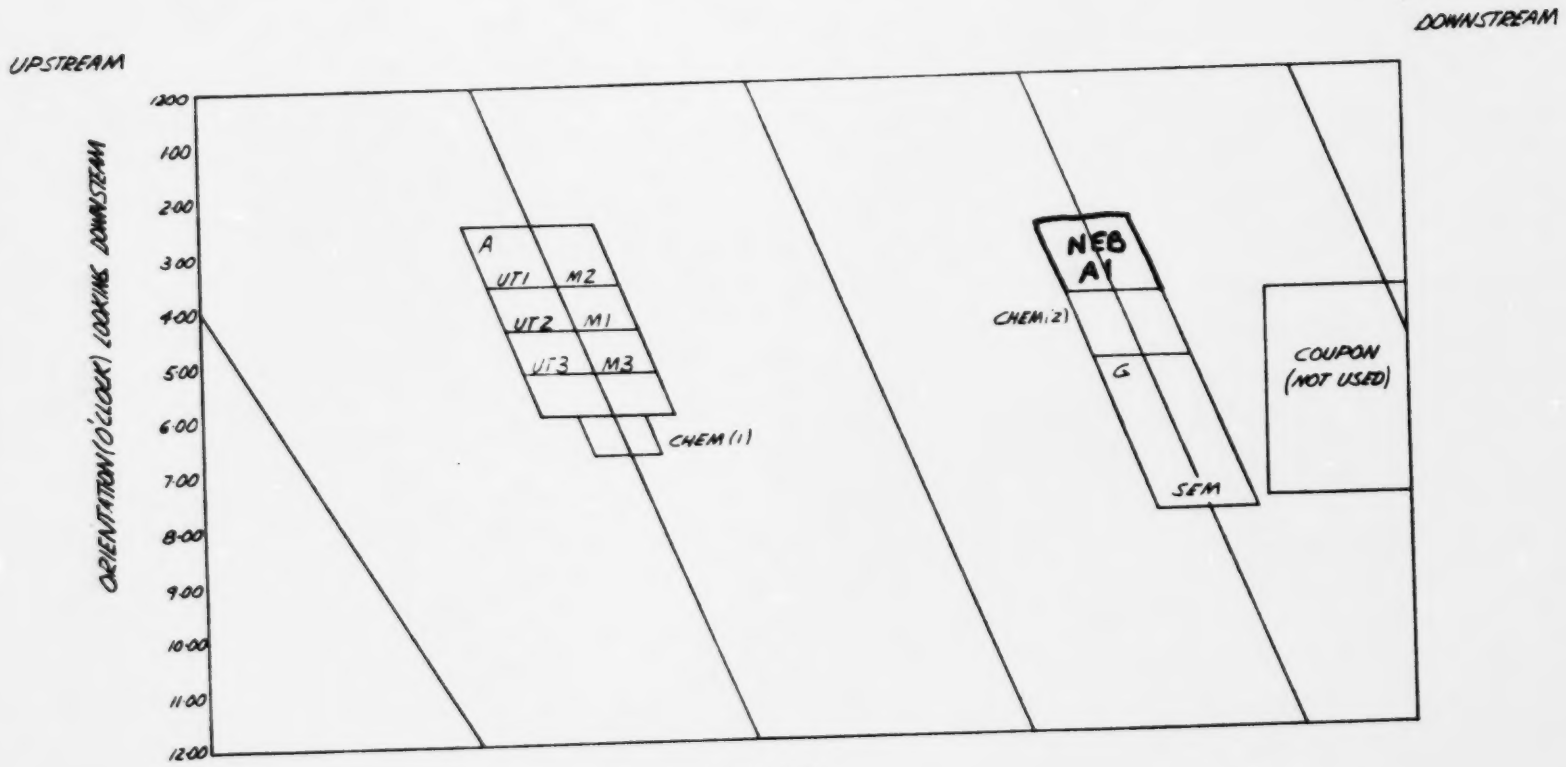

FIGURE (10)

MAP LOCATING COUPONS REMOVED FROM PIPE SECTION (A1).

PIPE A SECTION A2 (Failure No. 1, July 20)

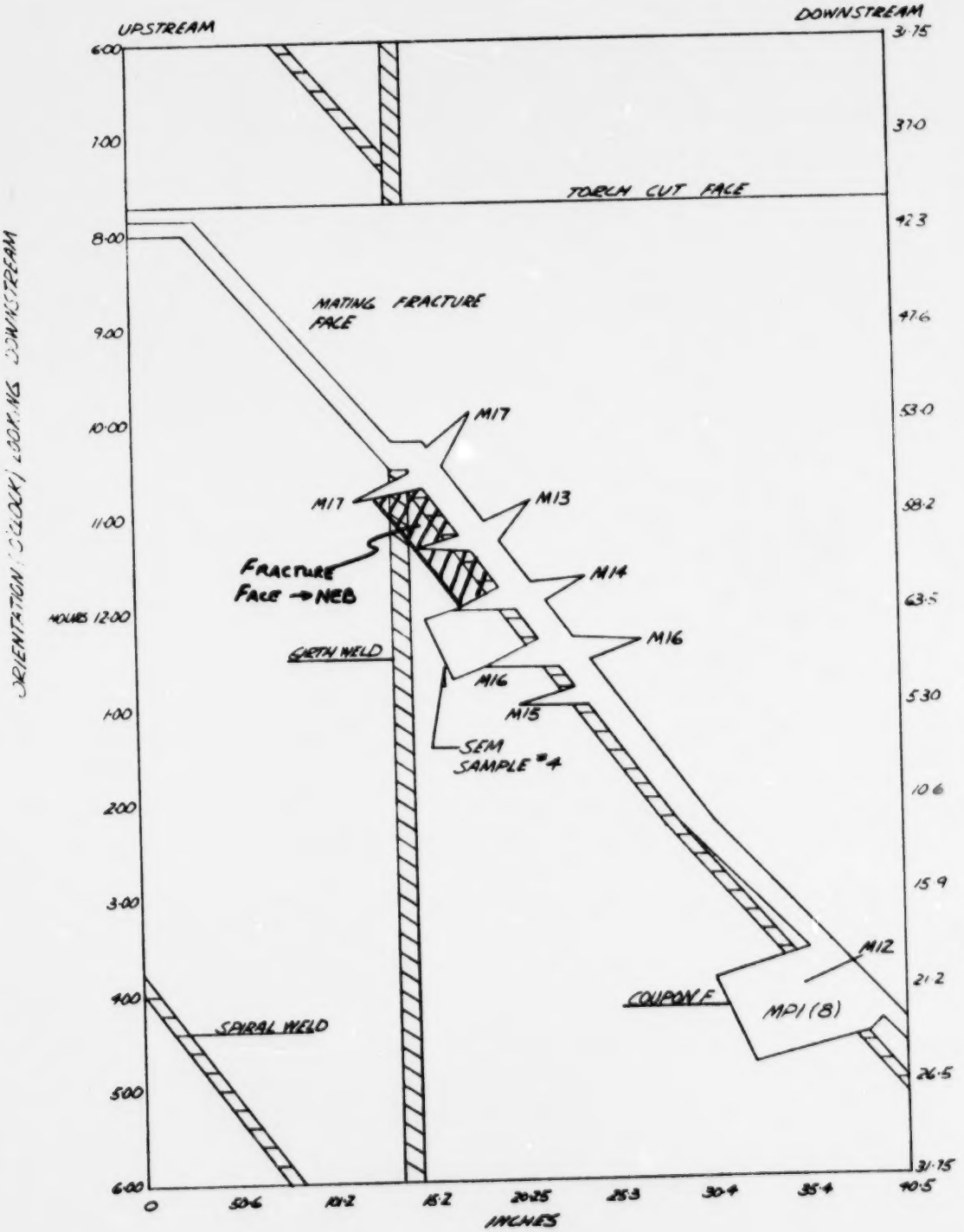

FIGURE (16)

MAP OF FRACTURE FACE, LOCATING COUPONS REMOVED FROM FRACTURE FACE REGION.

PIPE A SECTION A3 (Failure No. 1, July 20)

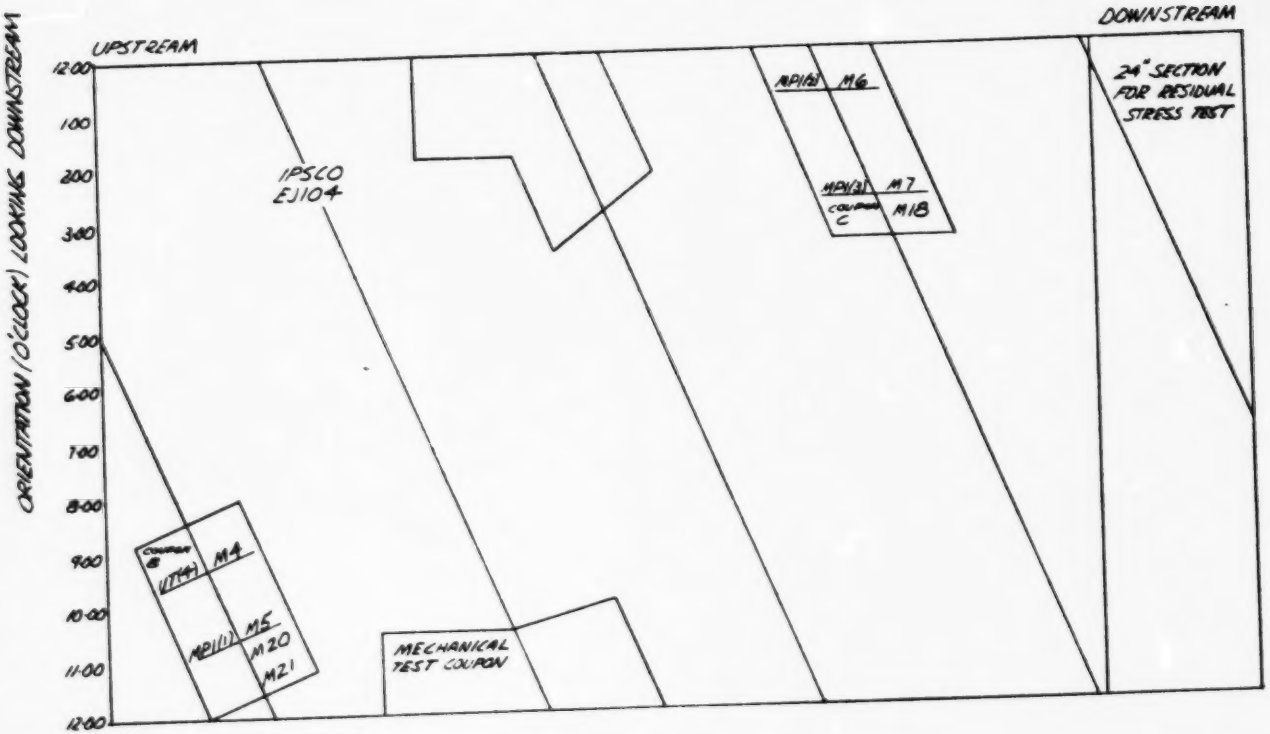

FIGURE (11)

MAP LOCATING COUPONS REMOVED FROM PIPE SECTION (A3).

PIPE B (Failure No. 1, July 20)

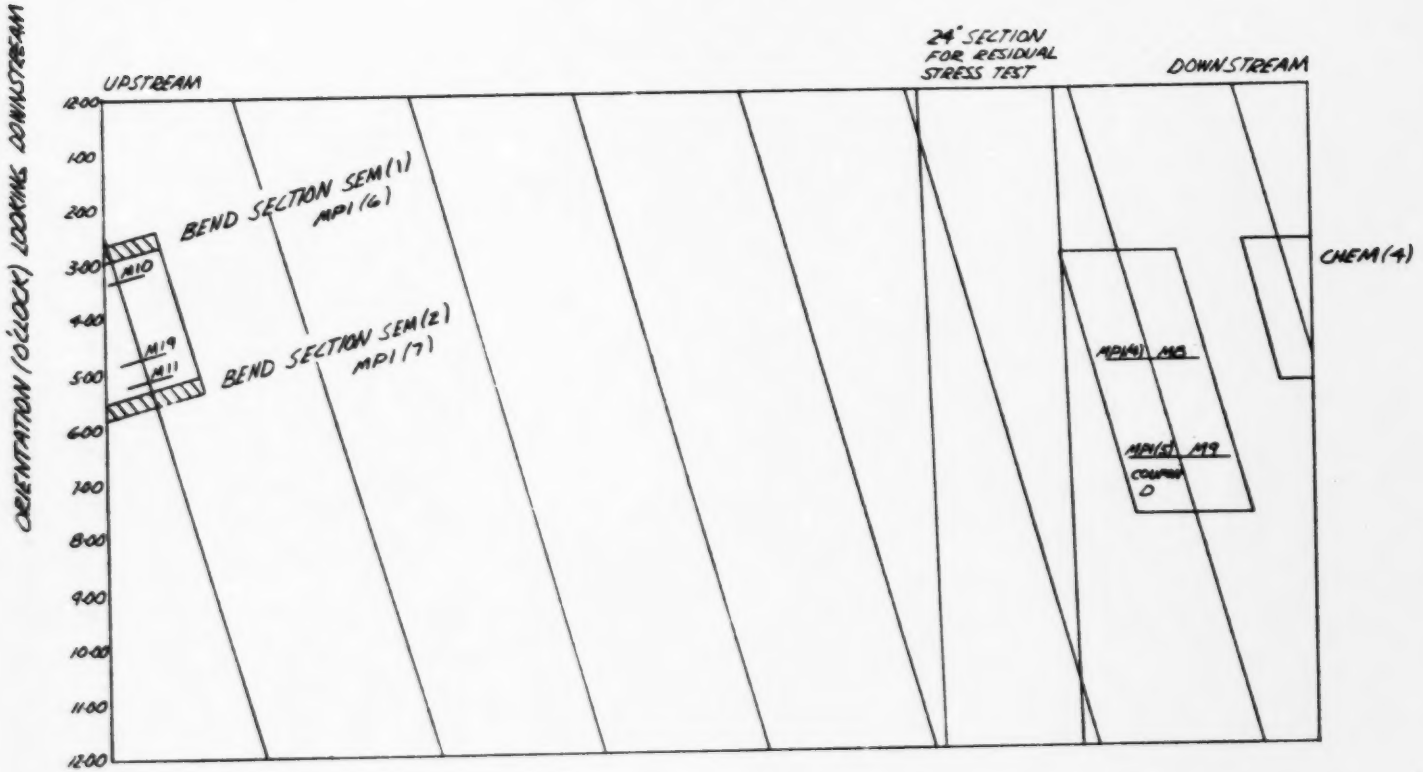

FIGURE (12)

MAP LOCATING COUPONS REMOVED FROM PIPE SECTION (B).

TABLE (VI) (Failure No. 1, July 20)

Chemical Analysis of Pipe and Weld Materials
From Location of Mechanical Test Coupon (A3)

Sample Location	Carbon Equivalent	Element (%) C	Mn	P	S	Si	Ni	Cu	Cr	Mo	Nb	V	Ti	Sn
Pipe (EJ104)	0.38	0.10	1.32	0.012	0.025	0.06	0.12	0.26	0.02	0.15	<0.10	<0.01	<0.01	<0.01
Outer Weld (Spiral)	0.40	0.12	1.33 1.36	0.013	0.011	0.15	0.09	0.23	0.02	0.11	<0.10	<0.01	<0.01	<0.01
Inner Weld (Spiral)	0.43	0.09	1.71 1.67 1.73	0.011	0.014	0.18	0.08	0.22	0.03	0.10	<0.10	<0.01	<0.01	<0.01
CSA Z 245.2 Standard	0.45 Max.	0.26 Max.	0.60 Min.	0.03 Max.	0.035 Max.	0.50 Max.	0.15 *	0.15 *	0.10 *	0.02 *	0.11 Max.	0.11 Max.	0.06 Max.	0.02 *

* Reportable

$$\text{Carbon Equivalent} = C + \frac{(Mn)}{6} + \frac{(Cr + Mo + V)}{5} + \frac{(Ni + Cu)}{15}$$

TABLE (VII) (Failure No. 1, July 20)

Chemical Analysis
Inner and Outer Weld Beads

Sample Location	Weld Bead	Carbon Equivalent	Element (%) C	Mn	P	S	Si	Ni	Cu	Cr	Mo	Nb	V	Ti	Sn
Failed Joint (EJ104) Mech.Test Coupon A3 from Table (VI)	Inner	0.43	0.09	1.71 1.67 1.73	0.011	0.014	0.18	0.08	0.22	0.03	0.10	<0.10	<0.01	<0.01	<0.01
	Outer	0.40	0.12	1.33 1.36	0.013	0.011	0.15	0.09	0.23	0.02	0.11	<0.10	<0.01	<0.01	<0.01
Failed Joint (EJ104) Location of Failure Coupon CHEM (FF)	Inner		0.11	1.73	0.014	0.024	0.25	0.08	0.21	0.03	0.14				
	Outer		0.09	1.23	0.019	0.022	0.25	0.08	0.19	0.04	0.13				
Failed Joint (EJ104) Downstream End Pipe (B) Coupon(CHEM 4)	Inner		0.07	1.74	0.010	0.015	0.26	0.09		0.04	0.11				
	Outer		0.09	1.46	0.015	0.005	0.25	0.12		0.03	0.18				
Joint Upstream of Failure. Upstream End Pipe (A1) Coupon (CHEM 1)	Inner		0.08	1.45	0.017	0.016	0.24	0.08		0.03	0.09				
	Outer		0.06	1.48	0.009	0.012	0.23	0.11		0.02	0.16				
Joint Upstream of Failure. Downstream End Pipe (A1) Coupon (CHEM 2)	Inner		0.10	1.42	0.011	0.011	0.23	0.15		0.03	0.15				
	Outer		0.10	1.47	0.014	0.032	0.21	0.19		0.02	0.13				
Joint Downstream of Bullmoose Tie-In. Upstream Joint, Pipe (C) Coupon (CHEM 5)	Inner		0.08	1.74	0.016	0.015	0.23	0.12	0.24	0.06	0.12				
	Outer		0.09	1.52	0.014	0.032	0.23	0.13	0.25	0.03	0.13				
Joint Downstream of Bullmoose Tie-In. Downstream Joint, Pipe (C) Coupon (CHEM 6)	Inner		0.08	1.40	0.009	0.025	0.19	0.12		0.04	0.11				
	Outer		0.10	1.41	0.012	0.020	0.22	0.15		0.02	0.15				

WESTCOAST 20" GRIZZLY
LINE EB-7-1004 (2ND FAILURE (Failure No. 2, July 27)

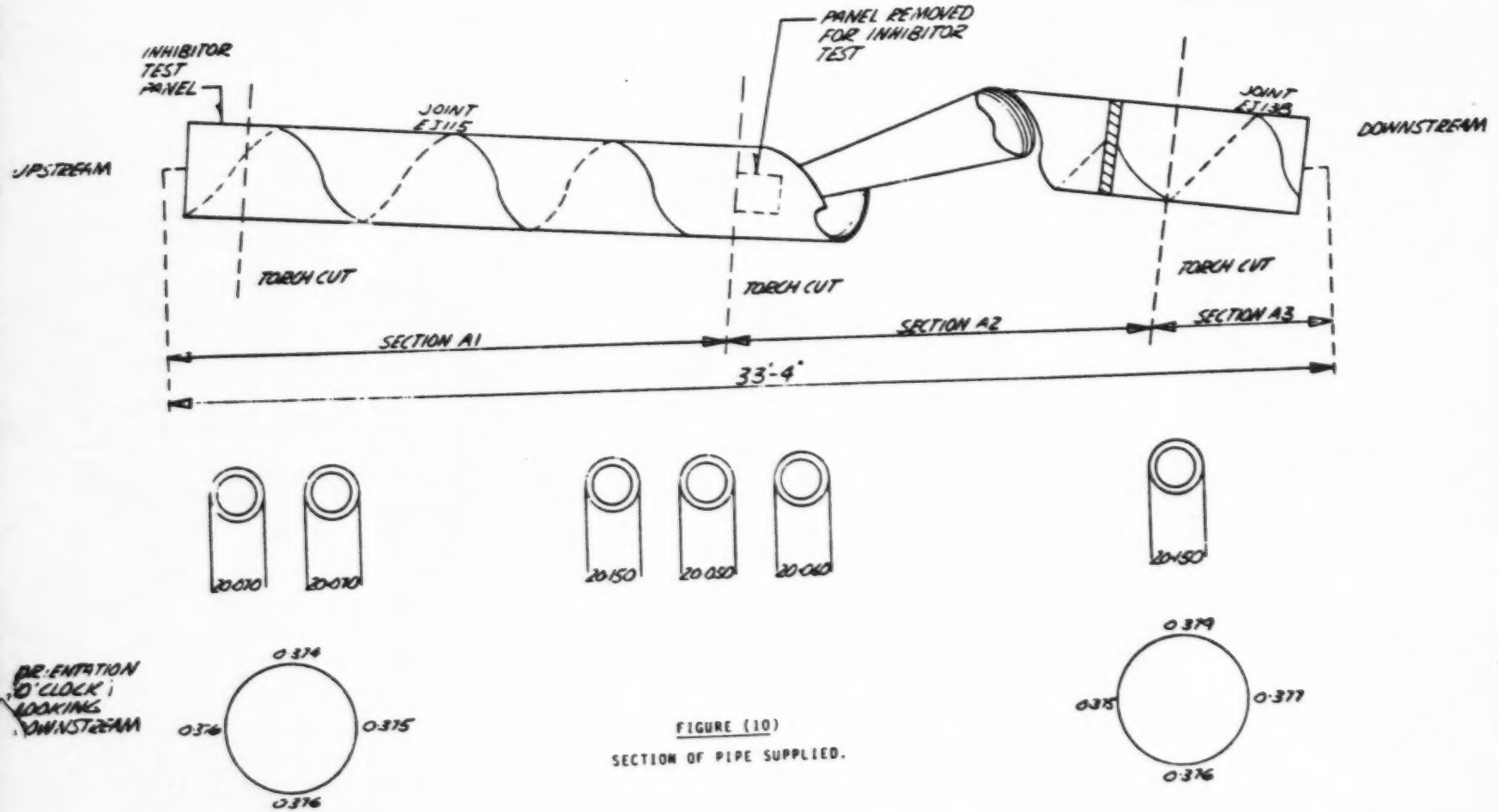

FIGURE (10)
SECTION OF PIPE SUPPLIED.

PIPE SECTION A1 (Failure No. 2, July 27)

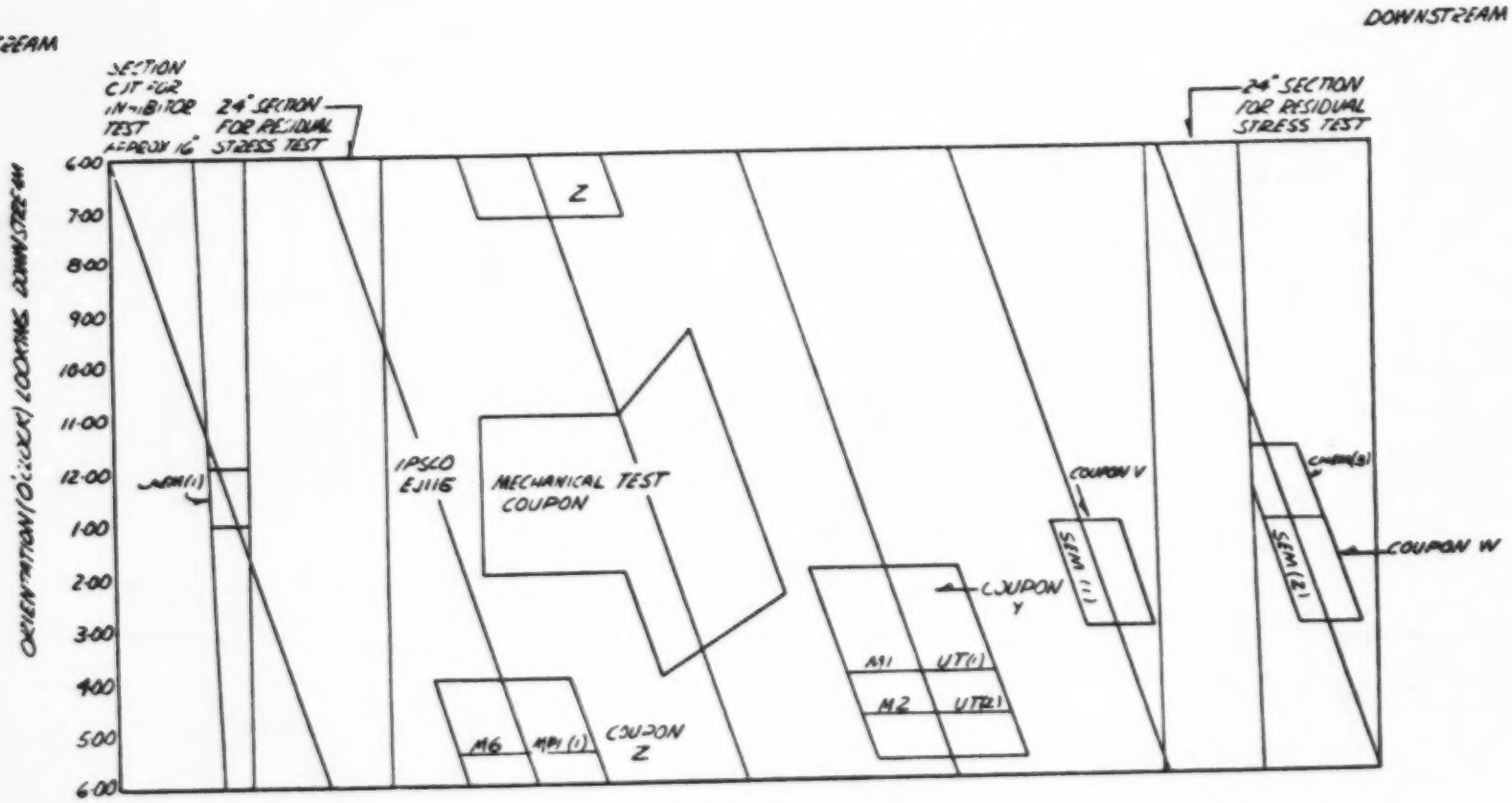

FIGURE (12)

MAP LOCATING COUPONS REMOVED FROM PIPE SECTION (A1).

PIPE SECTION A2 FRACTURE FACE (Failure No. 2, July 27)

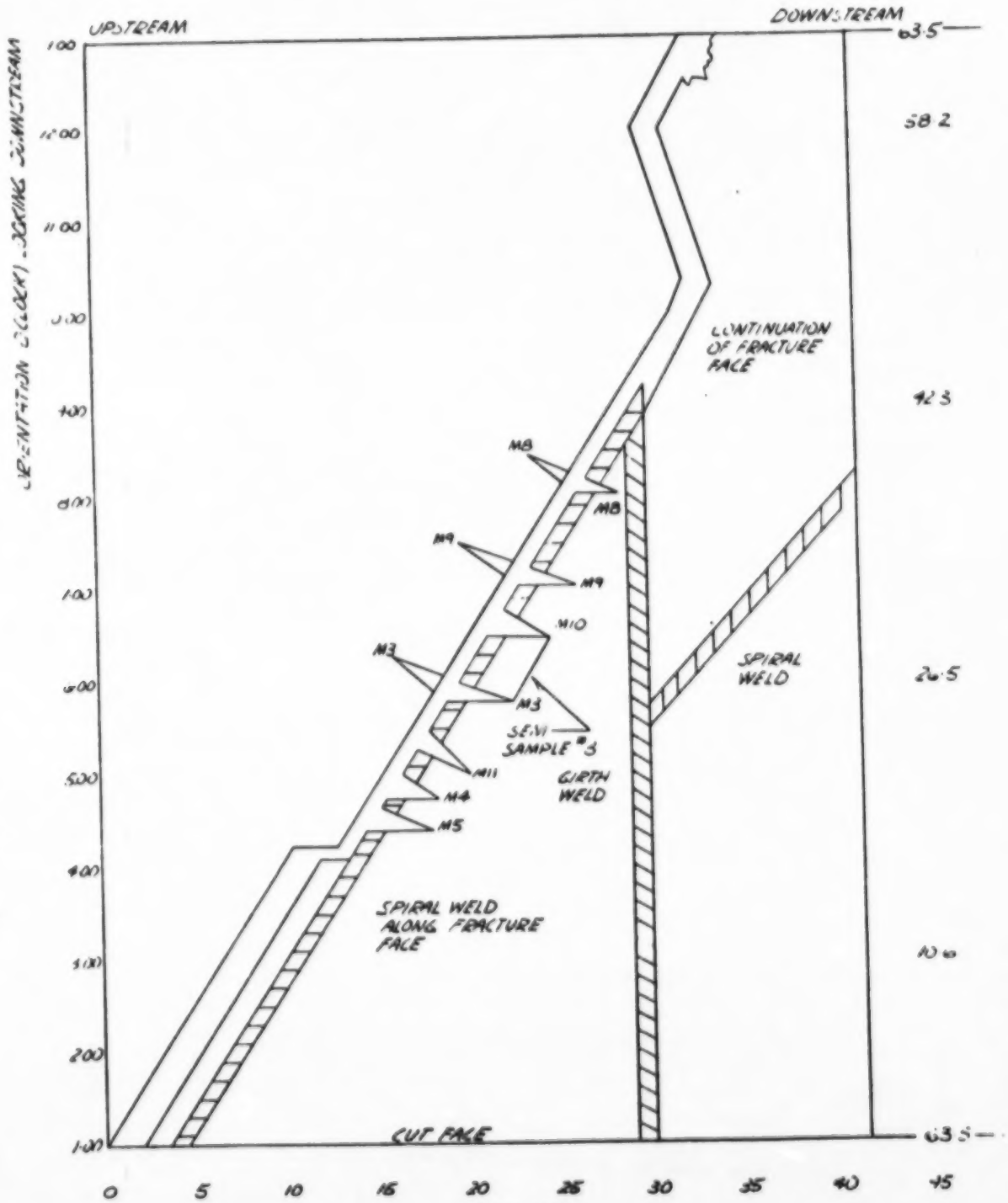

FIGURE (19)

MAP OF FRACTURE FACE, LOCATING COUPONS REMOVED FROM FRACTURE

PIPE A SECTION A3 (Failure No. 2, July 27)

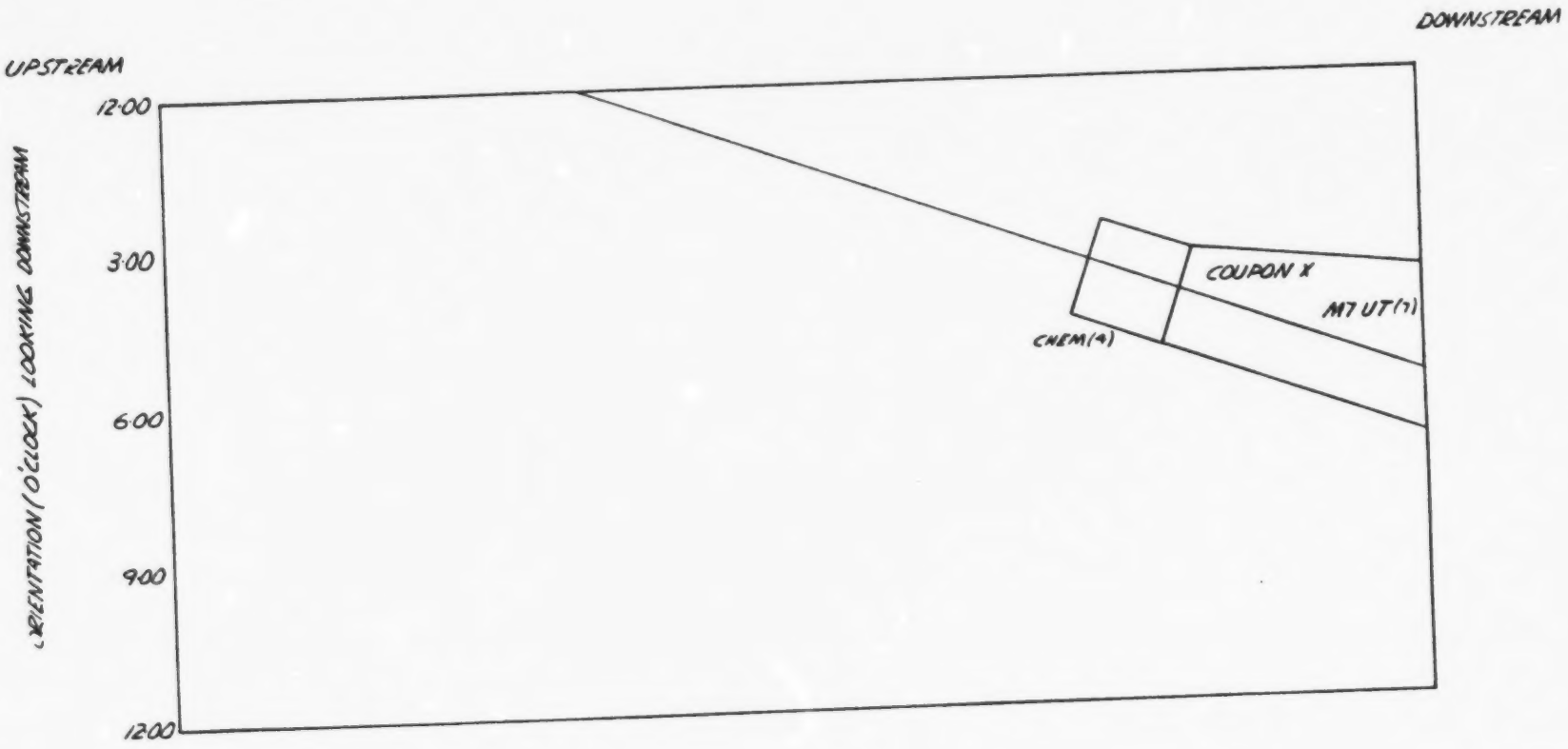

FIGURE (13)

MAP LOCATING COUPON REMOVED
FROM PIPE SECTION (A3).

TABLE (III) (Failure No. 2, July 27)

Chemical Analysis of Pipe and Weld Materials From Location of Mechanical Test Coupon (A1)

Sample Location	Carbon Equivalent	Element (%) C	Mn	P	S	Si	Ni	Cu	Cr	Mo	Nb	V	Ti	Sn
Pipe (EJ115)	0.36	0.09	1.27	0.010	0.030	0.03	0.11	0.22	0.02	0.16	<0.10	<0.01	<0.01	<0.01
Outer Weld (Spiral)	0.36	0.09	1.31 1.33	0.009	0.015	0.19	0.09	0.18	0.03	0.12	<0.10	<0.01	<0.01	<0.01
Inner Weld (Spiral)	0.41	0.08	1.68 1.61 1.69	0.016	0.015	0.21	0.08	0.18	0.03	0.12	<0.10	<0.01	<0.01	<0.01
CSA Z 245.2 Standard	0.45 Max.	0.26 Max.	0.60 Min.	0.03 Max.	0.035 Max.	0.50 Max.	0.15 *	0.15 *	0.10 *	0.02 *	0.11 Max.	0.11 Max.	0.06 Max.	0.02 *

* Reportable

$$\text{Carbon Equivalent} = C + \frac{(Mn)}{6} + \frac{(Cr + Mo + V)}{5} + \frac{(Ni + Cu)}{15}$$

TABLE (IV) (Failure No. 2, July 27)

CHEMICAL ANALYSIS, INNER AND OUTER WELD BEADS

Sample Location	Weld Bead	Carbon Equivalent	Element (%) C	Mn	P	S	Si	Ni	Cu	Cr	Mo	Nb	V	Ti	Sn
Failed Joint (EJ115) Upstream End Pipe (A1) Coupon (CHEM 1)	Inner		0.07	1.74	0.016	0.015	0.17	0.08		0.03	0.12				
	Outer		0.07	1.31	0.012	0.016	0.18	0.10		0.04	0.13				
Failed Joint (EJ115) Mech. Test Coupon (A1) From Table (III)	Inner	0.41	0.08	1.68 1.61	0.016	0.015	0.21	0.08	0.18	0.03	0.12	<0.10	<0.01	<0.01	<0.01
	Outer	0.36	0.09	1.69 1.31 1.33	0.009	0.015	0.19	0.09	0.18	0.03	0.12	<0.10	<0.01	<0.01	<0.01
Failed Joint (EJ115) Location of Failure Coupon (CHEM FF)	Inner		0.09	1.72	0.015	0.009	0.21	0.08	0.22	0.04	0.12				
	Outer		0.07	1.23	0.011	0.013	0.24	0.09	0.23	0.04	0.13				
Failed Joint (EJ115) Downstream End Pipe (A1) Coupon (CHEM 3)	Inner		0.07	1.74	0.010	0.007	0.21	0.09		0.02	0.13				
	Outer		0.09	1.27	0.011	0.016	0.23	0.09		0.03	0.12				
Joint Downstream of Failure (A3) (EJ138) Coupon (CHEM 5)	Inner		0.10	1.55	0.017	0.011	0.18	0.09	0.24	0.03	0.09				
	Outer		0.08	1.29	0.016	0.014	0.14	0.08	0.25	0.03	0.09				
Joint Downstream of Failure (A3) (EJ138) Coupon (CHEM 4)	Inner		0.10	1.68	0.018	0.010	0.22	0.10		0.03	0.10				
	Outer		0.09	1.43	0.013	0.008	0.19	0.10		0.03	0.08				